



UNDERGRADUATE DESIGN TEAM  
UNIVERSITY OF MARYLAND - COLLEGE PARK

35TH ANNUAL AMERICAN HELICOPTER SOCIETY  
INTERNATIONAL STUDENT DESIGN COMPETITION 2018

## Kwatee Design Proposal

*Sponsored by The United States Army Research Laboratory*





**Alfred Gessow Rotorcraft Center**  
Department of Aerospace Engineering  
University of Maryland  
College Park, MD 20740 U.S.A.

**Alexander Cheung**  
*Undergraduate Student (Team Lead)*  
ACheung2@terpmail.umd.edu

**Jonathan D. Detoro**  
*Undergraduate Student*  
Jdetoro713@gmail.com

**Havya H. Patel**  
*Undergraduate Student*  
Havya@terpmail.umd.edu

**Jason Xu**  
*Undergraduate Student*  
Jasonxu580@gmail.com

**Dr. James Baeder**  
*Faculty Advisor*  
Baeder@umd.edu

**Dr. Camli Badrya**  
*Faculty Advisor*  
Cbadrya@umd.edu

**Ian K. Bahr**  
*Undergraduate Student*  
Ikbahr26@gmail.com

**Westley R. Weinkam**  
*Undergraduate Student*  
Westweinkam@gmail.com

**Matthew C. David**  
*Undergraduate Student*  
Mdauid23@umd.edu

**Samuel B. Dame**  
*Undergraduate Student*  
Samdame9@gmail.com

**Dr. V.T. Nagaraj**  
*Faculty Advisor*  
Vnagaraj@umd.edu

*Students will receive credit for ENAE 482  
(Aeronautical Systems Design) for their  
contributions.*



**Alfred Gessow Rotorcraft Center**  
Department of Aerospace Engineering  
University of Maryland  
College Park, MD 20740 U.S.A.

**To the American Helicopter Society:**

The members of the University of Maryland Undergraduate Student Design Team hereby grant full permission to distribute the enclosed Executive Summary and Final Proposal for the 35th Annual Design Competition as they see fit.

Regards,

The UMD Undergraduate Design Team

# Acknowledgements

The University of Maryland Undergraduate design team would like to acknowledge the following people for their help throughout the duration of the 2018 AHS design competition. Thank you for your guidance and continued support.

## University of Maryland

*Dr. James Baeder* - Associate Professor, Dept. of Aerospace Engineering  
University of Maryland, College Park

*Dr. Vengalattore T. Nagaraj*- Senior Research Scientist, Dept. of Aerospace Engineering  
University of Maryland, College Park

*Dr. Inderjit Chopra* - Alfred Gessow Professor and University Distinguished Professor, Director of Alfred Gessow Rotorcraft Center, Dept. of Aerospace Engineering  
University of Maryland, College Park

*Dr. Bharath Govindarajan* - Asst. Research Professor, Dept. of Aerospace Engineering  
University of Maryland, College Park

*Dr. Camli Badrya* - Asst. Research Scientist, Dept. of Aerospace Engineering  
University of Maryland, College Park

## Special Thanks To:

Dylan Jude

Elena Shrestha

Stacy Sidle

Dr. Ananth Sridharan

Dr. Vikram Hrishikeshavan

Dr. Ashish Bagai

Brent T. Mills

---

# Contents

<b>Acknowledgment</b>	<b>viii</b>
<b>List of Figures</b>	<b>viii</b>
<b>List of Tables</b>	<b>x</b>
<b>1 Introduction</b>	<b>1</b>
1.1 RFP Analysis	1
1.1.1 RFP Requirements and Compliance	3
1.2 Vehicle Metrics Assessment	3
<b>2 Mission Requirements</b>	<b>4</b>
2.1 Multi-Mission Capabilities	5
2.2 Sizing Missions	5
2.2.1 Hover Based Mission: Search and Rescue	5
2.2.2 Forward Flight Based Mission: Disaster Relief and Telecommunication Restoration	6
<b>3 Vehicle Configuration Selection</b>	<b>7</b>
3.1 Selection Criteria: Analytical Hierarchy Process	7
3.1.1 Design Drivers	8
3.1.2 Design Driver Weights	9
3.2 Considered Configurations	10
3.3 Pugh Decision Matrix	10
3.4 Final Considered Configurations	11
3.4.1 Tail Sitter	11
3.4.2 Ducted Fan	11
3.4.3 Coaxial Rotor	12
3.5 Tailsitter Configuration Downselection	12
3.5.1 Wing Selection	12
3.5.2 Rotor Configuration	12
3.5.2.1 Winged Quadrotor Configuration	12
3.5.2.2 Coaxial Quadrotor	13
3.5.2.3 Main Proprotor Plus Quadrotors	13
3.5.2.4 Coaxial Main Proprotor	14
<b>4 Preliminary Vehicle Sizing</b>	<b>14</b>
4.1 Sizing Methodology	14
4.1.1 Rotor Sizing	15
4.1.2 Wing Sizing	15
<b>5 Blade Design</b>	<b>16</b>
5.1 Design Goals	16
5.2 Design Methodology	16
5.2.1 Baseline Airfoil Selection	17
5.2.2 Blade Twist and Taper	17

---

5.3	Rotor Blade Structural design . . . . .	19
5.4	Hub Design . . . . .	20
5.4.1	Blade Grip Design . . . . .	20
<b>6</b>	<b>Power System Overview</b>	<b>22</b>
6.1	Powerplant Selection . . . . .	22
6.1.1	Engine Operation . . . . .	23
6.1.2	Transmission . . . . .	23
6.2	Cooling System . . . . .	23
6.3	Lubrication System . . . . .	23
<b>7</b>	<b>Wing Design</b>	<b>24</b>
7.1	Box Wing Selection . . . . .	24
7.2	Airfoil Selection . . . . .	24
7.3	Taper Ratio . . . . .	25
7.4	Wing Structural Design . . . . .	25
7.4.1	Material Selection . . . . .	25
<b>8</b>	<b>Performance Analysis</b>	<b>26</b>
8.1	Hover Performance . . . . .	26
8.2	Drag Estimation . . . . .	26
8.3	Forward Flight Performance . . . . .	27
<b>9</b>	<b>Airframe Structural Design</b>	<b>28</b>
9.1	Load Paths . . . . .	29
9.2	Fuselage Structure . . . . .	30
9.3	Lower Wing Strut . . . . .	30
9.4	Hard Points . . . . .	31
9.5	Rotating Shroud . . . . .	31
9.6	Tail Fin . . . . .	31
9.7	Landing Gear . . . . .	31
9.7.1	Sealed Oleo – Pneumatic Strut Sizing . . . . .	32
9.8	Material Selection . . . . .	32
9.9	Mitigation of Lightning and Static Charges . . . . .	34
<b>10</b>	<b>Avionics</b>	<b>34</b>
10.1	Mission Requirements . . . . .	34
10.2	Sensor Suite . . . . .	35
10.2.1	Flight Control and Autonomy . . . . .	35
10.2.2	Flight Navigation and Communication . . . . .	36
10.2.3	Take-Off and Landing . . . . .	36
10.2.4	Supporting Equipment . . . . .	37
10.2.4.1	Avionics for Morphing and Reconfigurability . . . . .	37
10.3	Optional Equipment . . . . .	38
10.4	Placement of Avionics . . . . .	38
10.5	Avionics Weights and Power Requirements . . . . .	39
<b>11</b>	<b>Flight Dynamics and Control</b>	<b>39</b>

---

11.1 Flight Dynamics Model . . . . .	39
11.2 Control Scheme . . . . .	40
11.2.1 Hover and Forward Flight Maneuver . . . . .	40
11.2.2 Transition . . . . .	40
11.3 Empennage Sizing . . . . .	43
11.4 Static Stability . . . . .	43
<b>12 Acoustics</b>	<b>44</b>
<b>13 CONOPS</b>	<b>45</b>
13.1 Basis for Concept of Operations . . . . .	45
13.2 Cargo Loading . . . . .	45
13.3 Intelligence, Surveillance, Reconnaissance (ISR) . . . . .	47
13.4 Transportation and Ground Safety . . . . .	47
13.5 Maintenance . . . . .	47
<b>14 Cost Analysis</b>	<b>47</b>
14.1 Production Costs . . . . .	47
<b>15 Weight Breakdown</b>	<b>48</b>
<b>16 Summary</b>	<b>50</b>
<b>Bibliography</b>	<b>51</b>

---

# List of Figures

- 1.1 Relative Size Comparison of R22, PA-28 and *Kwatee* . . . . . 3
- 2.1 *Kwatee* Flying Above a Disaster Area . . . . . 7
- 3.1 Weights of Design Drivers . . . . . 9
- 3.2 Designs That Represent Each Considered Configuration . . . . . 10
- 3.3 Final Considered Configurations . . . . . 11
- 3.4 Pros and Cons of Quadrotor Configuration . . . . . 12
- 3.5 Pros and Cons of Coaxial Quadrotor Configuration . . . . . 13
- 3.6 Pros and Cons of Main Rotor Plus Quadrotor Configuration . . . . . 13
- 3.7 Pros and Cons of Coaxial Main Proprotor Configuration . . . . . 14
- 4.1 Team Developed Flowchart Showing Sizing Code Convergence . . . . . 15
- 5.1 Geometry of *Kwatee*'s Blade Choice . . . . . 17
- 5.2 *Kwatee*'s Airfoil Comparison in Hover and Forward Flight . . . . . 18
- 5.3 Progression of Twist and Taper Analysis . . . . . 19
- 5.4 Rotor Blade Cross Section . . . . . 19
- 5.5 Fan Plots for Hover (a) and Axial Flight (b) . . . . . 20
- 6.1 Specific Power vs. Fuel Consumption for Possible Engines . . . . . 23
- 6.2 Engine Intake and Exhaust . . . . . 24
- 7.1 Wing Airfoil and Profile Lift vs Angle of Attack Characteristics . . . . . 25
- 7.2 Cross section of the wing . . . . . 26
- 8.1 Power Required vs. Axial Velocity . . . . . 28
- 8.2 Distance per kg Fuel vs. Axial Velocity . . . . . 28
- 9.1 The four main sections of *Kwatee* . . . . . 28
- 9.2 Load paths during forward flight . . . . . 29
- 9.3 Load paths during hover . . . . . 29
- 9.4 Load paths on ground . . . . . 29
- 9.5 A strut attaching the lower wing to the fuselage . . . . . 30
- 9.6 Tie down attachment points . . . . . 31
- 9.7 Rotating shroud that covers up the ducts during axial flight . . . . . 31



---

9.8	Internal structure of the tail fin . . . . .	32
9.9	Landing gear attachment . . . . .	32
10.1	Avionics Flow Chart . . . . .	35
10.2	LIDAR Sweep to a 3 m Diameter . . . . .	36
10.3	Avionic Placement . . . . .	38
11.1	Hover . . . . .	40
11.2	Forward Flight . . . . .	40
11.3	Locations of Control Mechanisms . . . . .	40
11.4	<i>Kwatee's</i> Continuous-ascent Transition and Transition Free Body Diagram . . . . .	41
11.5	Body Pitch Angle (a) vs time and Velocity vs time (b) . . . . .	42
11.6	Required Thrust vs time (a) and $C_L$ vs time (b) . . . . .	42
11.7	<i>Kwatee's</i> Complete Flight Path . . . . .	43
11.8	Moment Equilibrium for Static Stability . . . . .	44
13.1	Door providing access to the engine bay . . . . .	47
15.1	<i>Kwatee Weight Chart</i> . . . . .	49

# List of Tables

1.1 RFP Compliance . . . . .	3
1.2 Comparison of Basic Sizing Metrics for of Kwatee with Comparable Size Commercial Aircraft . . . . .	4
1.3 RFP Performance Metrics of Compared Aircraft . . . . .	4
3.1 Design Driver Selection . . . . .	8
3.2 Pugh Decision Matrix . . . . .	10
4.1 Comparison of Basic Sizing Metrics for Analyzed Designs . . . . .	16
5.1 Comparison of Basic Sizing Metrics for Analyzed Designs . . . . .	18
6.1 Comparison of Engine Types for Powerplant Selection . . . . .	22
7.1 Wing Geometry . . . . .	26
8.1 <i>Kwatee's</i> Hover Time with 50% Fuel Burn . . . . .	26
8.2 Breakdown of Drag Contributions . . . . .	27
8.3 Summary of Forward Flight Performance Metrics (100kg fuel) . . . . .	28
10.1 Avionics Breakdown . . . . .	39
11.1 Mechanisms for Desired Maneuvers . . . . .	40
14.1 Production Costs ** Fuel cost based on prices as of May, 2018 . . . . .	48
15.1 CG Position (From Top of Aircraft) . . . . .	48



# Introduction

The 35th Annual Student Design Competition, the American Helicopter Society Request for Proposal (RFP) is to design a Group 3 size Unmanned Aerial Systems (UAS) with Vertical Takeoff and Landing (VTOL) capabilities. Group 3 is defined by the U.S. Department of Defense (DoD) as an unmanned vehicle under 600 kg. The design will incorporate a novel reconfigurable design capable of efficient hover and fast forward flight. The goal is to create an aircraft with superior performance over comparable sized aircraft, which do not have reconfigurable design capable of operating in a megacity-type environment. To be able to navigate down narrow streets and in confined spaces, the maximum size in hover of the vehicle must be no larger than 3 m by 3 m square. The requirements and their solution are tabulated in Table 1.1 and further discussed below.

## 1.1 RFP Analysis

The RFP requires the following:

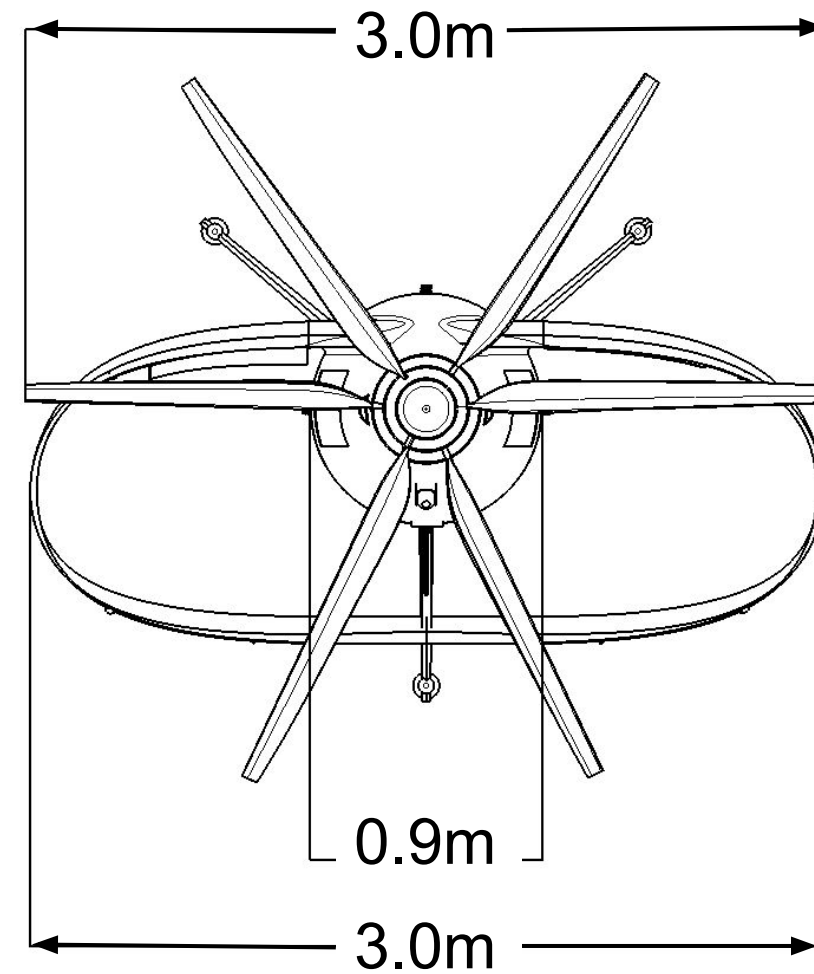
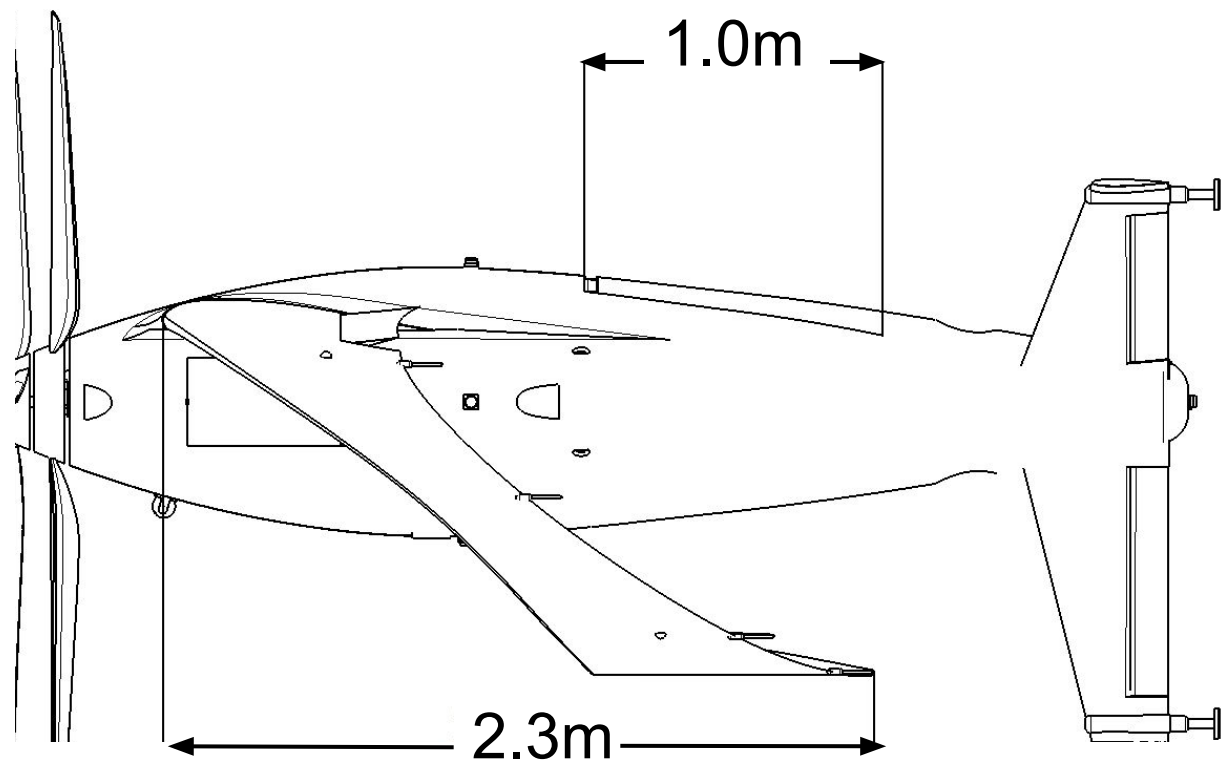
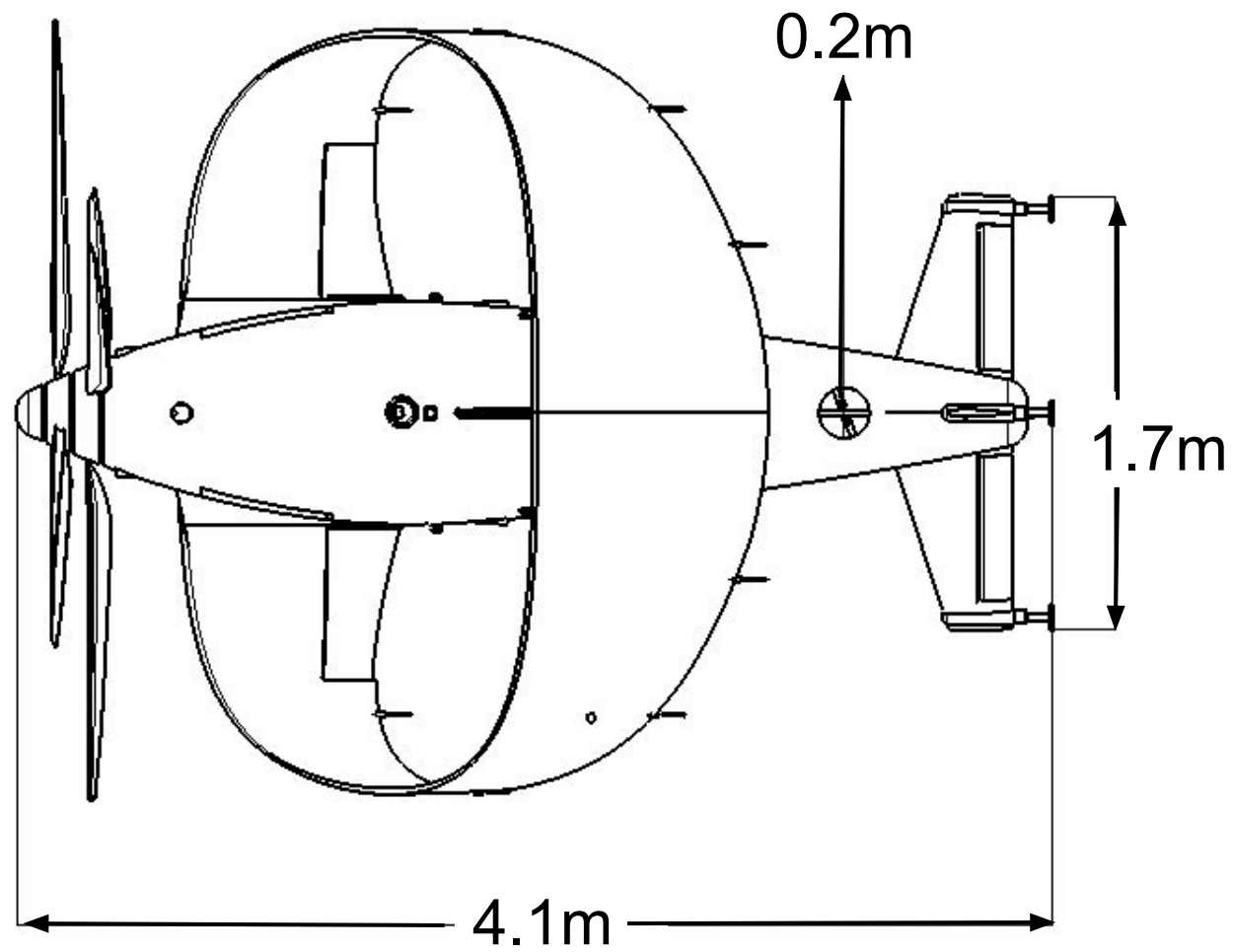
- The main lifting device must be reconfigurable. As defined by the RFP, reconfigurability is a system or component that is capable of performing in two different modes; with each mode being able to either change shape, orientation, or location of component relative to the fixed body frame. Each mode should be shown to have particular trade offs in performance that is not present in the other mode. The choice of each operating configuration will correspond to specific flight conditions and the optimal performance desired, hover or forward flight. Also the reconfigurable system is the focus of the novel design and a key feature of the VTOL aircraft. The aircraft must be able to reconfigure between two different operating modes on its own and all effort to change between states must be by components onboard the aircraft at all times; at no point can a component be jettisoned or removed.
- During transitioning, the aircraft should be stable and controllable at all times. Design cannot be prior VTOL designs; the design must be new and novel. Past VTOL designs may be used if the performance can be improved by the use of new technology that was originally unavailable during the initial design.
- New technologies may be incorporated into the design as long as there is public documentation, i.e. journal papers, conference proceedings, or technical reports, with descriptions of performance and properties. Such technology shall not be the main focus of the design, but it can be the key feature that enables the aircraft to be capable of the transitioning between the two states.

In response to the RFP, the *Kwatee* is the innovative design and novel configuration developed by the University of Maryland Undergraduate Design Team. To highlight the spirit of reconfigurability and the United States Army tradition of using names with Native American origin, the name *Kwatee* was selected; the cheerfully optimistic Native American God of transformation and improvement, from the northwestern Nootka, Puget, and Quinault tribes.

*Kwatee* is a novel coaxial proprotor tailsitter utilizing a variable incidence box wing. The space efficient box wing and coaxial proprotor are used to take full advantage of the limited space of the 3 m by 3 m size constraint in hover, acting as a tail-sitter (see 3-View Drawing fold-out). Utilizing most of the area available for the rotor allows for lowering the disk loading, creating the safest possible conditions for ground operations and allows *Kwatee* to hover efficiently within the constraints of the RFP.



# Kwatee 3-View Drawing



The variable incidence wing allows for a zero lift angle of attack when in hover mode, while maintaining an optimally trimmed angle of attack in forward flight. The box wing provides similar lift and reduces the induced drag as a larger span wing, thus lowering the required power to produce the same axial thrust. The transition between the hover mode and forward flight mode is achieved using a ducted fan embedded in the rear-end of the fuselage, lowering the total time and power required for the transition. All of these important features are detailed later in the report, as shown by the section numbers in Table 1.1.

### 1.1.1 RFP Requirements and Compliance

TABLE 1.1: RFP Compliance

RFP Requirement	Design Solution	RFP Sections
Max Size of 3m x 3m in hover	Utilized a box wing and coaxial proprotor in tailsitter configuration capable of producing more lift in a smaller span	2.2.4
Reconfigurable	Novel variable incidence box wing and ducted tail fan enables smooth transition between hover and forward flight modes	2.2.1
Efficient Hover	Coaxial rotor allows for maximum disk area and no tail rotor, resulting in lower disc loading and high power loading	2.2
Fast Forward Flight	Low weight fuel-efficient twin turboshaft engine, along with low induced and profile drag from box wing and fuselage with excellent fineness ratio	2.2
Unmanned vehicle	Advanced avionics package allows for fully autonomous missions	2.2

## 1.2 Vehicle Metrics Assessment

During the design process, benchmarks were created based off of the similarly sized helicopter (Robinson R22) and a fixed wing aircraft (Piper PA-28 Cherokee) seen in Figure 1.1. With the goal to design a Group 3 UAS, the RFP states certain design and performance constraints, which the proposal must follow: Max Takeoff Weight, Operating Altitude, Maximum Airspeed, Payload, and Maximum Vehicle Span. From Table 1.2 it can be seen that even with the constraints of a smaller gross takeoff weight and smaller footprint *Kwatee* was able to outperform comparable aircraft.

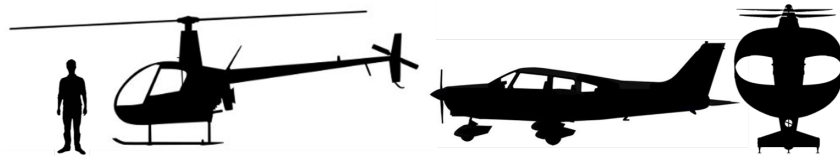


FIGURE 1.1: Relative Size Comparison of R22, PA-28 and *Kwatee*

For performance comparison with existing successful commercial aircraft, four characteristics are used: (1) hover time in hours at sea-level standard altitude (SLS) and at 3000 m standard atmosphere

TABLE 1.2: Comparison of Basic Sizing Metrics for of Kwatee with Comparable Size Commercial Aircraft

	RFP	R22	PA-28	<i>Kwatee</i>
Maximum Gross Takeoff Weight (MTOW)	600 kg (1300 lbs)	635 kg	975 kg	<b>533 kg (1172 lbs)</b>
Operating Altitude standard atmosphere	3,000 m (9,900 ft)	4,267 m	4,267 m	<b>3,000 m (9,900 ft)</b>
Maximum Airspeed ( $V_{\max}$ )	335 km/h (180 knots) or greater	188.9 km/h	227.8 km/h	<b>425 km/h (230 knots)</b>
Payload	100 kg (220 lbs) or greater	218 kg	430 kg	<b>100 kg (220 lbs)</b>
Maximum Vehicle Span (in hover)	3 m (9.8 ft)	7.67 m	9.2 m	<b>3 m (9.8 ft)</b>

consuming 50% of energy capacity (fuel, batteries, etc), (2) cruise range at velocity for best range ( $V_{BR}$ ) consuming 50% of energy capacity at SLS and 3000 m, (3) Dash speed ( $V_{MAX}$ ) at SLS and 3000 m, and (4) estimated Drag Area which is defined as:

$$DragArea = \frac{DragForce}{\frac{1}{2}\rho V_{MAX}^2}$$

Table 1.3 shows how these aircraft compare with the performance metrics described in RFP.

TABLE 1.3: RFP Performance Metrics of Compared Aircraft

	R22	PA-28	<i>Kwatee</i>
Endurance	2 hours	2.5 hours	<b>SLS: 1.74 hours 3000 m: 1.45 hours</b>
Cruise Range	193 km (104.3 NM)	475 km (256.3 NM)	<b>SLS: 510 km (281 nm) 3,000 m: 515 km (278 NM)</b>
Dash speed ( $V_{\max}$ )	188.9 km/h	227.8 km/h	<b>SLS: 389 km/h 3000 m: 425 km/h</b>
Estimated Drag Area	0.8 m <sup>2</sup>	0.77 m <sup>2</sup>	<b>0.16 m<sup>2</sup></b>

## Mission Requirements

The RFP does not state a specific mission, but instead focuses on the design being capable of efficient hover and fast forward flight for civilian based missions. It states the need for the UAS to be capable of navigating within a megacity environment, which may contain an urban canyon. An urban canyon is characterized as streets flanked by buildings on both sides creating conditions similar to a canyon.



This is highlighted in the RFP requirements to restrict the horizontal span of the vehicle to 3 meters, similar size to the width of a standard city lane, while in hover mode. For forward flight, the UAS needs to be capable of maximum dash speed of 425 km/h (230 knots), which is faster than most similar sized civilian fixed wing aircraft. This combination of capabilities, efficient hover and fast forward flight, lends itself to missions focusing on disaster relief.

## 2.1 Multi-Mission Capabilities

*Kwatee* is designed to be used for civilian based missions with a focus on extended range and endurance that will highlight the hover and forward flight capabilities of the UAS. With these features in mind, the designed missions will focus on disaster relief. *Kwatee* will be able to deliver emergency supplies to remote areas affected by natural disasters (as shown in Figure 2.1), scan disaster areas for lost and stranded civilians, and help establish and restore emergency communications after a disaster.

**Disaster Resupply:** During or after a disaster, *Kwatee* will be capable of reaching remote areas that are not accessible by other means of transportation. It will be able to deliver emergency medical supplies and rations to assist emergency recovery.

**Search and Rescue:** *Kwatee* will monitor activity above a disaster area and be able to facilitate search and rescue missions. For this, the main payload will be surveillance and avionics equipment to help locate lost and stranded civilians. With a launch location near the disaster zone *Kwatee* will be capable of traveling to the disaster zone in forward flight mode and with its extended endurance will scan over the region using a thermal infrared and optical surveillance suite. In addition, once located a minimal survival package can be delivered (cell phone, water, first aid kit, blanket).

**Telecommunications:** *Kwatee* can act as a mobile communication network to restore cellular services and provide help to victims. *Kwatee* will carry communications gear capable of relaying radio and cell transmissions to and from a disaster zone. With its expanded range and hovering capabilities, *Kwatee* will travel from outside a disaster zone and land on top of a high rise building. Then deploy communications gear to restore mobile service.

## 2.2 Sizing Missions

Based on the RFP requirements, *Kwatee* will operate in two distinct flight modes: hover and forward flight. *Kwatee* is being designed with adaptability for multiple flight missions with the capability to support a variety of payloads. The example missions are emblematic of this desire and derived from the RFP requirement for *Kwatee* to be operable in narrow streets and confined spaces. The hover-based flight mode is designed to fulfill the RFP requirement of hover time at 50% energy consumption. While the forward flight based mission is designed to showcase the potential cruise range for *Kwatee*. Together the two flight modes signify the potential for this design to fulfill different mission profiles as well as use its reconfigurability to optimize its performance in different flight regimes. The missions below are examples of hover and forward flight based mission profiles.

### 2.2.1 Hover Based Mission: Search and Rescue

A search and rescue based mission is designed to support the performance metric of Hover-time in hours consuming 50% of energy capacity. The payload for this mission will consist of a supplemental avionics package designed to provide increased thermal infrared and optical capabilities to locate lost and or stranded civilians as well as additional fuel for increased hover duration.



1. **Pre-Flight:** After all pre-flight checks have been completed *Kwatee* can start-up and idle on ground for 5 minutes. During this time, the onboard computer will perform its default sensor calibration and pre-flight check process of its components. Furthermore, the ground station will either upload the mission profile to the onboard computer or establish connection for remote piloting feature. By the end of this idle time, *Kwatee* is ready for takeoff.
2. **Takeoff and Climb:** *Kwatee* will takeoff then begin climbing immediately to the operating altitude of 3,000 m (9843 ft) ISA. The climb rate and time for this section of the mission profile will be based on the powerplant size selected. However, climb rate is not a direct performance metric so it will not be a direct driver for powerplant size.
3. **Cruise:** *Kwatee* will transition from hover to forward flight configuration then proceed to the desired Surveillance area or city. This range and time will also be derived from the powerplant size, but are more crucial than the climb rate. The range and time for this section will consume approximately 15% of the total fuel and will be conducted at velocity for best range (VBR).
4. **Hover:** *Kwatee* will transition from forward flight to hover configuration then proceed as instructed in the onboard mission or through remote piloting inputs. This section of the mission will consist of pure hover at an operating altitude anywhere between 3,000 m and sea level. This section of the mission will directly drive the size of the powerplant as this is a direct RFP requirement and will consume at least 50% of the fuel capacity. Optional minimal survival package can be delivered if lost or stranded civilians are found.
5. **Repeat Cruise:** *Kwatee* will transition from hover to forward flight configuration and head back to the base at VBR and consume approximately 15% of total fuel reserve.
6. **Descent and Landing:** Upon completion of the final cruise aspect of the mission, *Kwatee* will transition from forward flight to hover configuration and descend from the operating altitude 3,000 m (9843 ft) ISA to SL. After landing, *Kwatee* will idle to cool down the engine and perform a final systems check to determine if any maintenance operations are needed before applying the rotor brake and engine shutdown.

### 2.2.2 Forward Flight Based Mission: Disaster Relief and Telecommunication Restoration

Disaster resupply and telecommunications based missions are dominated by forward flight and designed to support the performance metric of Cruise Range at  $V_{BR}$  consuming 50% of energy capacity. The payload for disaster resupply mission would consist of medical supplies, emergency rations, and water. This type of mission shows *Kwatee* could be used to support first responders and provide help to hurricane areas as seen in Houston post hurricane Harvey (see Figure 2.1).

1. **Pre-Flight:** Follow the pre-flight routine as described in Section 2.2.1.
2. **Takeoff and Climb:** Follow the takeoff and climb profile as described in Section 2.2.1.
3. **Cruise:** *Kwatee* will transition from hover to forward flight configuration then proceed to the desired location either loaded into the navigation computer or by remote pilot input. This aspect of the mission will consume between 25-35% of the fuel capacity.
4. **Hover:** *Kwatee* will transition from forward flight to hover configuration and descend to drop location or sea level depending upon mission requirements. *Kwatee* will then land and drop payload in either one or multiple locations during this segment of the mission. This portion of





the mission will have the largest range in fuel consumption due to the possibilities of dropping payload in multiple locations but will maximize at 20%. However, depending on the range, if only dropping at one location, *Kwatee* can support a large payload at a cost of less fuel.

5. **Repeat Cruise:** After dropping the payload, *Kwatee* will immediately ascend back to 3000 m then repeat Step 3 and return to base at VBR with fuel consumption of 25-35%.
6. **Descent and Landing:** After reaching base, *Kwatee* will resume hover configuration and descend from operating altitude of 3,000 m (9843 ft) ISA to SL. After landing, *Kwatee* will idle engine and perform final systems check before rotor slowing and engine shutdown.

These missions were designed to show the multi-mission capability of the *Kwatee* design as well as translate the design capabilities to the RFP requirements. Many other potential civilian and military missions can be envisioned, including non-urban environments. For all missions, the operating altitude is stated as 3,000 m, but the vehicle will be designed to operate anywhere between sea level and 3000 m. maximizing targeted values for hover-time, VBR, cruise range, etc. were the determining factors for the final configuration and powerplant selection.



FIGURE 2.1: *Kwatee* Flying Above a Disaster Area

## Vehicle Configuration Selection

After reviewing the RFP, and an initial trade-off study, it was concluded that the configuration for the design must be a compound configuration that is capable of reconfiguring to provide optimal performance during different mission stages. The possible configurations considered for the design were: single main rotor, tilt rotor, tail sitter, multirotor, ducted fan, coaxial, synchropter, spinning body, distributed thrust, cyclopter, stop rotor, notar, and tip-jet. The configurations were then compared to each other through multiple sets of Pugh Matrices using the analytical hierarchy process.

### 3.1 Selection Criteria: Analytical Hierarchy Process

During the design selection the Analytical Hierarchy Process (AHP) was used to narrow down the selection process. This was used extensively during the creation of the design drivers (Table 3.1) and

helped prioritize the relative importance in conjunction with the RFP. AHP is a technique of relating each design choice in a pairwise comparison to select the best choice, taking into account objective and subjective opinions from the group. This allowed the team to methodically prioritize which decisions would most directly impact vehicle performance and the RFP.

### 3.1.1 Design Drivers

The RFP outlined three main goals for the design: efficient hover, fast forward flight, and new and novel reconfigurable design. From this, additional design drivers were created with the goal to optimize customer satisfaction and be a base for design considerations. From the three main requirements of the RFP, 18 possible design drivers were created. These criteria were based off the specific requirements of the RFP as well as other criteria created by the team. From the initial list of design drivers, items were eliminated or combined to reach the final 8 design criteria based on relevance to the mission profiles. This was accomplished by the team members individually ranking the importance of the proposed design drivers to the three main requirements of the RFP. Each design driver was evaluated for its individual importance, from a scale of 1 to 5, and compared to the design criteria set by the RFP. The results were tabulated and included the average value and standard deviation as seen in Figure 3.1.

TABLE 3.1: Design Driver Selection

	Innovation	Versatility	Transportability	Hover Efficiency	Controllability	Technology	Reliability	Cost	Durability	Safety	Fast Forward Flight	Safety of environment	Manufacturability	Operability	Payload Capability	Operation Cost	Range	Agility	
Total	Novel	35	20	15	19	14	22	12	13	12	11	22	12	14	14	18	10	18	19
	Hover	21	23	10	35	26	18	18	10	16	17	8	18	12	22	23	12	20	28
	Fast Forward Flight	23	23	8	9	24	18	17	10	13	13	35	13	11	20	23	13	27	25
Avg	Novel	4.375	2.5	1.875	2.375	1.75	2.75	1.5	1.625	1.5	1.375	2.75	1.5	1.75	1.75	2.25	1.25	2.25	2.375
	Hover	2.625	2.875	1.25	4.375	3.25	2.25	2.25	1.25	2	2.125	1	2.25	1.5	2.75	2.875	1.5	2.5	3.5
	Fast Forward Flight	2.875	2.875	1	1.125	3	2.25	2.125	1.25	1.625	1.625	4.375	1.625	1.375	2.5	2.875	1.625	3.375	3.125
STD DEV	Novel	0	1.464	1.215	1.496	1.414	1.069	1.254	1.215	0.951	0.976	1.215	1.113	0.816	1.291	1.512	0.535	1.512	1.38
	Hover	1.155	1.496	0.787	0	1.254	1.134	1.272	0.787	1.113	1.134	0.378	1.397	1.254	1.069	0.756	0.756	1.069	0.816
	Fast Forward Flight	1.113	1.496	0.378	0.488	0.976	1.272	0.976	0.787	1.464	0.9	0	1.215	0.976	0.9	0.756	0.9	0.69	1.134
	<b>STD DEV</b>	<b>1.261</b>	<b>1.424</b>	<b>0.926</b>	<b>1.789</b>	<b>1.396</b>	<b>1.136</b>	<b>1.179</b>	<b>0.926</b>	<b>1.161</b>	<b>1.024</b>	<b>1.758</b>	<b>1.244</b>	<b>0.995</b>	<b>1.155</b>	<b>1.071</b>	<b>0.73</b>	<b>1.221</b>	<b>1.207</b>
	<b>Total</b>	<b>79</b>	<b>66</b>	<b>33</b>	<b>63</b>	<b>64</b>	<b>58</b>	<b>47</b>	<b>33</b>	<b>41</b>	<b>41</b>	<b>65</b>	<b>43</b>	<b>37</b>	<b>56</b>	<b>64</b>	<b>35</b>	<b>65</b>	<b>72</b>

Design drivers with large standard deviations were then reevaluated between the team members until a consensus was made. Some design drivers were eliminated because of the low importance relating to the mission profiles and RFP. Certain design drivers were very similar and thus were condensed with other drivers to create a more coherent overall design objective. The final eight design drivers are explained below:

- **Innovation:** The RFP states the design needs to be new and novel; this means the design cannot be based on current existing aircraft, however, the aircraft can use technology not available during original conception of past design configurations in order to increase performance or efficiency. Considered technologies must be publicly documented through analysis or testing. Individual technological innovations will not be the focus, but might be necessary to enable the aircraft to have its reconfigurable design. Selected technologies should improve performance and efficiency.
- **Versatility:** Create a platform that is capable of a wide variety of mission profiles. Consideration for possible missions that take full advantage of being autonomous, with efficient hover and extended range of an aircraft with fast forward flight. The Group 3 restriction will allow the

aircraft to be able to be transported by light utility vehicle. Being able to be deployed quickly and easily in many environments will add to the versatility in different applications.

- **Hover Efficiency:** Maximize power loading (Thrust/Power) to increase endurance in hover. Consider fuel and power needed to increase hover time. Ability to perform mission safely with a larger payload.
- **Controllability:** The ability for the aircraft to transition smoothly between hover configuration and fast forward flight configuration. Be able to takeoff, land, and maintain controlled hover in mega city environment with wind effect and strong gust. Capable of maintaining fast forward flight in cruise and full control during maneuvers.
- **Operation/Cost:** Total cost for development, testing, building, and maintaining aircraft will impact the design of the vehicle. The ease of manufacture includes machining cost, material availability and time to produce. The expense of each mission as well as routine maintenance needs to be considered as well as ease of training personnel, quick mission prep and takeoff. Consistent performance required over the lifetime of operations. Aircraft will complete missions in hostile/hazardous environments.
- **Durability:** A measure of robustness to withstand environmental conditions, abnormal flight conditions, and extended use during operation. Possibly consider flight worthiness during combat situations, if military version desired.
- **Safety:** When operating in confined space, it is important to have lower ground effect to minimize impact due to surrounding environment. Be able to withstand impacts or sudden changes to flight conditions. Be able to land safely after loss of power away from ground personnel and or inability to reconfigure from forward flight to hover. Include safety of civilians and those operating on the ground.
- **Fast Forward Flight:** Have a maximum range and dash speed greater than comparable sized VTOL. Be able to maneuver while maintaining fast forward flight. Increasing distance the craft can travel combined with the amount of time in station.

### 3.1.2 Design Driver Weights

After the establishment of the final design drivers the relative importance of each design driver was rated in relation to the RFP and to each other through the Analytical Hierarchy Process (AHP). This was done to determine the design drivers that were critical to the success of a mission versus ones that were not mission critical. A Pugh matrix was used to weigh each design driver's importance compared to the others. The results were then tabulated and normalized to one (1), giving individual weights to each of the design drivers (see Figure 3.1). From this analysis, the focus of the design will be focused on efficiency in hover and forward flight, but with innovation and controllability also playing key roles.

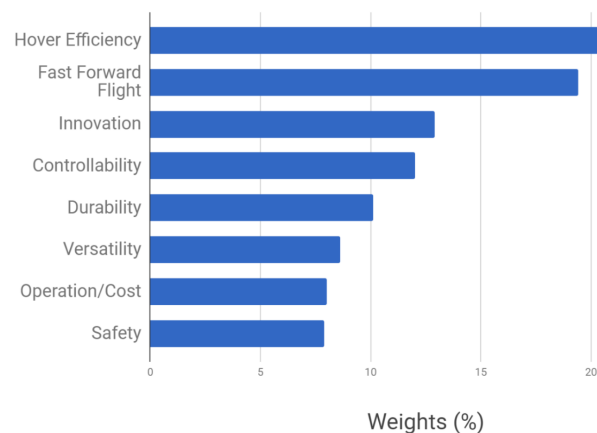


FIGURE 3.1: Weights of Design Drivers

### 3.2 Considered Configurations

In order to achieve the goals set forth by the customer, a brief study of popular designs was made early on in our design process to determine the components of each design that might be beneficial for the final design. Table 3.1 is a brief list of some of the aircraft examined are contained at the top of Table 3.2. An image of each design considered can be seen in Figure 3.2. Hovering is an important requirement of the RFP and a number of conventional and novel VTOL designs were considered. Therefore a traditional fixed wing design was not considered for a possible configuration.



FIGURE 3.2: Designs That Represent Each Considered Configuration

### 3.3 Pugh Decision Matrix

A Pugh Matrix was used to narrow down the configurations to a final few that will be researched further (see Table 3.2). This method involved each configuration to be graded on how it meets the requirements of each of the selected design drivers. This process was repeated till the results converged on the configurations with the most applicability to the goals of the RFP.

Each team member implemented the Pugh Matrix independently by comparing each configuration against the design driver and gave it a grade on a scale from -3 to 3 corresponding to the relative improvement over the baseline configuration, the single main rotor. The results were then averaged, tabulated, and totaled to give each configuration a ranking in order to see which configurations would be the focus of further research. The top three contenders are highlighted in dark green in Table 3.2.

TABLE 3.2: Pugh Decision Matrix

	Weight	SMR	tilt rotor	tail sitter	multi rotor	ducted fan	coaxial	synchropter	spinning body	cyclopter	stop rotor	notar	tip-jet
<b>Innovation</b>	0.129	0	1.032	0.903	0.774	1.032	1.161	1.290	1.548	1.161	0.258	0.258	0.516
<b>Versatility</b>	0.086	0	1.290	0.774	0.774	1.118	0.516	0.516	0.258	0.258	0.086	0.172	-0.602
<b>Hover Efficiency</b>	0.211	0	-2.743	1.055	2.100	2.954	2.321	2.321	0.422	1.899	-0.422	1.055	-1.688
<b>Controllability</b>	0.120	0	-0.960	-0.240	1.800	0.960	1.372	-0.120	-1.200	1.320	-0.480	0.480	-1.440
<b>Operation/Cost</b>	0.080	0	-0.880	0.480	-0.954	-0.320	-0.560	-0.800	0.160	-0.880	-0.800	-0.240	-0.400
<b>Durability</b>	0.101	0	-0.303	0.606	-0.431	0.606	-0.010	-0.606	-0.606	-0.505	-0.707	0.000	-1.111
<b>Safety</b>	0.079	0	-0.158	0.237	-0.131	1.027	1.567	-0.553	-0.553	0.140	0.158	0.869	-1.027
<b>Fast Forward Flight</b>	0.194	0	2.522	3.298	-0.196	1.552	0.970	0.000	0.970	0.388	2.716	0.388	-0.194
Total	1.000	0	-0.200	7.113	3.736	8.929	7.337	2.048	0.999	3.781	0.809	2.982	-5.946

### 3.4 Final Considered Configurations

With the completion of the Pugh matrix, the possible considered configurations were narrowed down to three final configurations: tail sitter, ducted fan, and coaxial rotor. Each configuration has its own advantages and drawbacks in regards to the RFP. To achieve the goal of fast forward flight and efficient hover the final design will need to take in attributes from each considered configuration in a compound design. A comparison of the three configurations are shown in the spider plot of Figure 3.3.

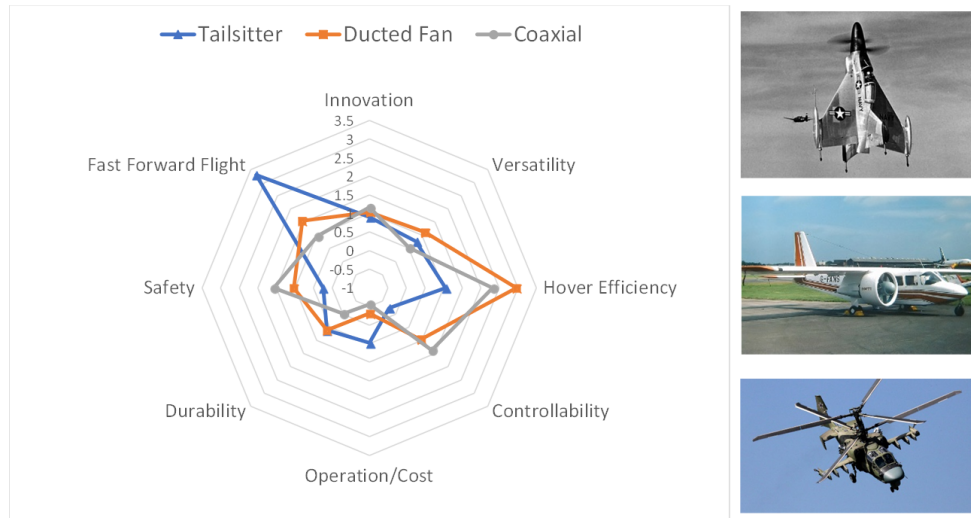


FIGURE 3.3: Final Considered Configurations

#### 3.4.1 Tail Sitter

The tailsitter combines the forward flight capability of a fixed-wing aircraft with the hovering capability of a rotary-wing aircraft. A tail sitter offers significant advantages over other VTOL aircraft with its ability to transform, by changing orientation, into a traditional forward flight airplane with corresponding maximum speed, range, and endurance. Furthermore, the fuselage can be longer than 3 m to enable an appropriate fineness ratio. One main drawback to all tail sitters is the additional systems and controls required to rotate the vehicles orientation. These additional transitional maneuvers to rotate the vehicle is more complex than traditional maneuvers performed by both conventional fixed wing and conventional rotorcraft, and will require a more complex system for the transition.

#### 3.4.2 Ducted Fan

A ducted fan configuration can be very efficient in hover allowing for efficient hover and the ability to navigate in a megacity environment. In addition, the shrouded rotors are extremely safe for ground crews working with or near the aircraft. Furthermore, ducted fans have similar advantage of vertical take off and transition into a faster, more efficient forward flight, compared to a tailsitter. However, this advantage comes at the cost of higher disk loading because of their smaller diameter propellers which results in high downwash. This higher downwash is an unfavorable performance metric in a urban canyon and for nearby people and property. There is also large parasitic drag in forward flight from the rotor shroud.

### 3.4.3 Coaxial Rotor

Coaxial configurations are also being considered due to the numerous advantages over other traditional VTOLs. There is no need for an anti torque mechanism, this allows for the overall system to be more compact than traditional rotorcraft. A coaxial design will also increase payload of a similar sized single rotor. One drawback of a coaxial rotors is the increased mechanical complexity of the rotor hub, this will also increase the overall weight and size.

## 3.5 Tailsitter Configuration Downselection

### 3.5.1 Wing Selection

For lift in forward flight, a biplane configuration was chosen early in the design process due to increased wing planform area within the permitted 3 m span, and potential for quadrotor hubs as mentioned below. While multiple rotor hubs were not part of *Kwatee*'s propulsion system, the benefits of dual wings led to a modified biplane design to remain as the final wing selection.

A monowing design is both lighter and has less profile drag compared to a biplane design. However, the low aspect ratio resulting from the limited span leads to very poor lift efficiency. The resulting high wing loading would also lead to poor low speed stability and undesirable stall characteristics. A biplane design mitigates many of these issues, at the cost of increased weight and profile drag. To address these issues, a box wing configuration was chosen. This novel wing design greatly reduces induced drag, and increases rigidity by structurally connecting upper and lower wingtips with box wing sides.

### 3.5.2 Rotor Configuration

The following rotor configurations were analyzed in combination with a boxed wing: quadrotor, coaxial quadrotor, proprotor and quadrotor, and coaxial proprotor. The pros and cons of each configuration are detailed in the following sections.

#### 3.5.2.1 Winged Quadrotor Configuration

A quadrotor configuration was analyzed in Figure 3.4 because it is a well known design that incorporates impressive hover maneuverability with reasonable axial forward flight propulsive qualities. Moreover, the quadrotor offers inherent redundancy in both hover and forward flight configurations. On the other hand, this configuration requires high blade tolerance as the radii grow towards the max span limit. The resulting power required for this configuration was considered too high to be viable; therefore, this configuration was dropped.

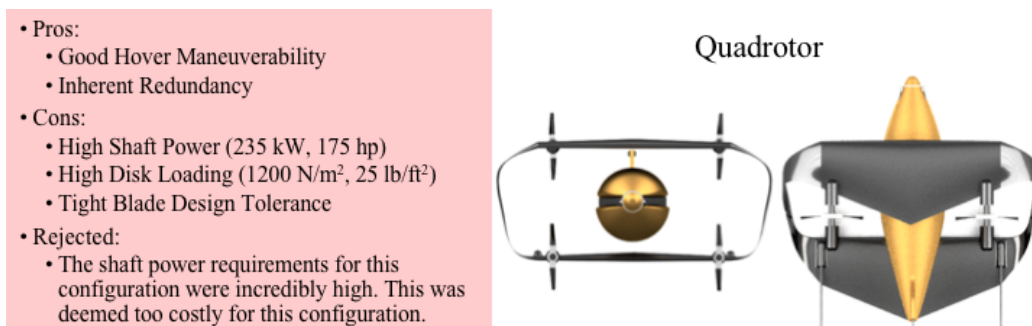


FIGURE 3.4: Pros and Cons of Quadrotor Configuration

### 3.5.2.2 Coaxial Quadrotor

The next configuration, coaxial quadrotor, (Figure 3.5) provides a solution to the large power required for the standard quadrotor. This configuration has similar controllability in hover and forward flight by modulating the RPM of different rotors. However, this configuration still has an incredibly high disk loading (DL). The high DL would decrease the hover efficiency for this configuration. Also, this DL would cause a high downwash at the landing site creating a potentially hazardous environment for people and property. This is even more critical in a mega-city environment that could be full of pedestrians; therefore, this configuration was also dropped.

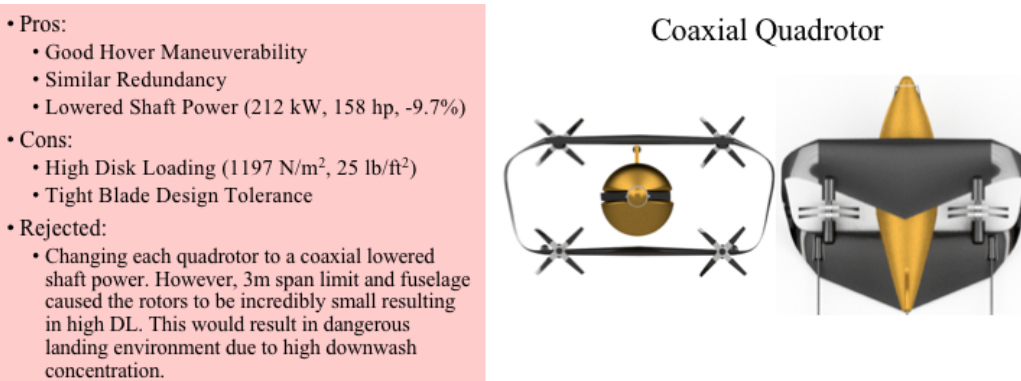


FIGURE 3.5: Pros and Cons of Coaxial Quadrotor Configuration

### 3.5.2.3 Main Proprotor Plus Quadrotors

One method of reducing DL was to add a main rotor in front of the fuselage. This increased the total rotor area within the 3 m span constraint by moving the quads to the edges and the main rotor occupied the middle of an effective 3 m square. This provided the lowest DL of any configuration as seen in Figure 3.6. Unfortunately, this design resulted in poor yaw control in hover. The quadrotor system could not produce enough torque to completely counter the effects of the main rotor. Some solutions were analyzed to combat this effect. The first was rotating all quadrotors in the same direction to counter torque in hover but this would have resulted in a roll imbalance in forward flight once the main rotor was feathered and the quadrotors provided the full thrust. The second solution considered was tilting two of the quad rotors down to mimic the effects of a tail rotor. This solution was not acceptable because the degree of tilt needed was 58° which would have required extensive structural support on the wings. None of these solutions were deemed viable due to power and weight penalties; therefore, this configuration was also dropped.

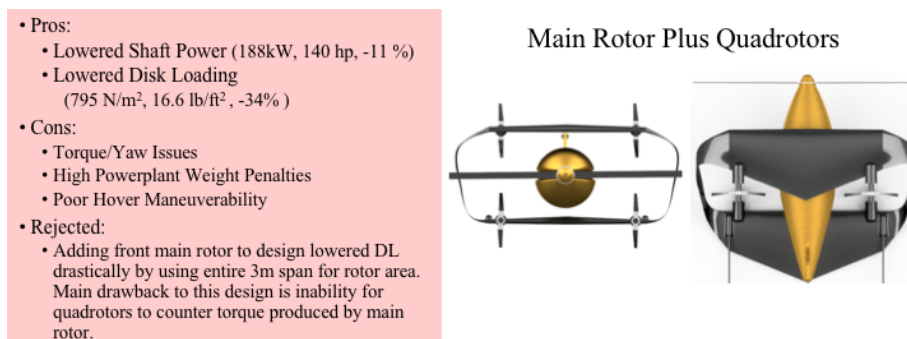


FIGURE 3.6: Pros and Cons of Main Rotor Plus Quadrotor Configuration

### 3.5.2.4 Coaxial Main Proprotor

In order to counter the torque and simplify the design, a coaxial main proprotor (Figure 3.7) was analyzed next. This configuration lowered the power required slightly but also raised the disk loading. The coaxial still has full maneuverability in hover with full cyclic and collective controls. Having the wing and the tail section within the induced flow, *Kwatee* will also experience better control characteristics while flying at low speeds due to improved flow over control surfaces. One potential issue was the transition to axial flight from hover. This issue was solved by adding a small ducted fan near the tail to provide a moment arm and allowing the wing to have a similar variable incidence (see Section 11.2.2) to provide constant lift and thus a smooth axial transition. Overall this configuration had the lowest power, low disk loading, full maneuverability and relatively simple powerplant structure; therefore, this configuration was chosen.

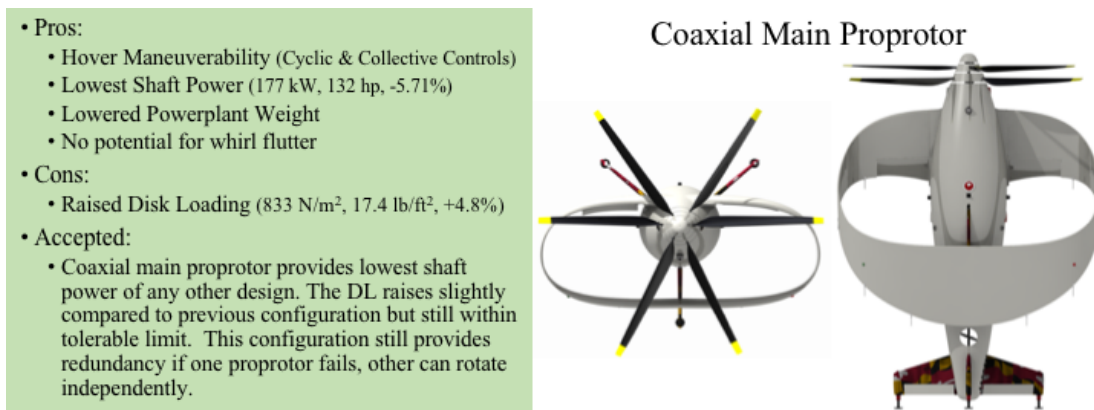


FIGURE 3.7: Pros and Cons of Coaxial Main Proprotor Configuration

## Preliminary Vehicle Sizing

An in-house sizing code was developed based on Tishchenko's methodology [1] with blade element momentum theory to model aerodynamics in hover and high speed axial forward flight. Due to the sizing constraints of 600 kg MTOW, 3 m span, and 100 kg payload, the sizing code progressed backwards from these design constraints. This year's RFP did not include a specific mission so *Kwatee* was designed with multi-mission capability. The missions described in Section 2 were used to size *Kwatee*.

### 4.1 Sizing Methodology

For the purpose of aerodynamic sizing, the potential rotor configurations for *Kwatee* were analyzed within the tailsitter regime in Section 3.5. Potential tailsitter rotor configurations were analyzed using the RFP design limitations on maximum span, MTOW,  $V_{\max}$  and minimum payload as seen in Figure 4.1. Using these limitations, the preliminary sizing code swept through key input parameters such as configuration and mission parameters then returned performance metrics: rotor power, disk loading, power loading, figure of merit (FM) and propulsive efficiency ( $\eta$ ). This was deemed the most appropriate method for analyzing potential designs to maximize hover and propulsive efficiency while keeping power required and powerplant weight minimum.



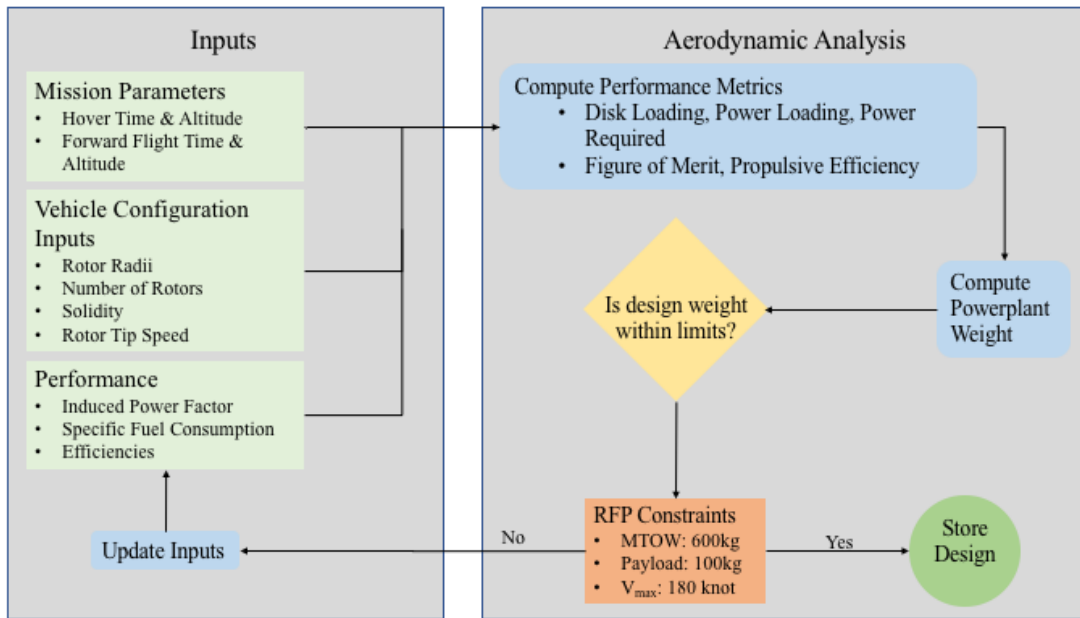


FIGURE 4.1: Team Developed Flowchart Showing Sizing Code Convergence

### 4.1.1 Rotor Sizing

Using the methodology outlined in Figure 4.1, different rotor configurations were analyzed for the tailsitter base. The mission parameters of hover time and forward flight time caused FM and propulsive efficiency ( $\eta$ ) to be weighted differently. The vehicle configuration inputs progressed as the different designs were analyzed as seen in Section 3.5. The performance inputs used average values for different types of engines including: turboshaft, diesel and rotary engines to provide an initial understanding of powerplant choices for each mission. A more detailed analysis of the engine comparisons and sizing is discussed in Section 6.1.

Based on the 3 m span restriction, a key design driver for preliminary sizing was the disk loading. The disk loading metric provided a qualitative understanding of the intensity of the downwash and the relative brownout caused by *Kwatee*'s rotor system. Due to the nature of *Kwatee*'s missions (Section 2) and the need to operate in a mega-city environment, the disk loading needed to be minimized while maintaining the 3m span limitation. Lowering the disk loading had a further effect on *Kwatee* by increasing the power loading and decreasing the power required. The power loading metric provides an understanding of the autorotative ability of *Kwatee* as well as hovering performance when compared to other helicopters. As seen in Table 4.1, *Kwatee*'s final rotor configuration with coaxial main rotor provides the lowest power required, 132 hp, and a low disk loading, 833 N/m<sup>2</sup> (17.4 lb/ft<sup>2</sup>), for the 3 m span limitation. This low power required allows for the lowest powerplant weight per mission time of any other rotor configuration analyzed.

### 4.1.2 Wing Sizing

The 3 m span limitation from the RFP not only provided a limitation on the rotor sizing but also on the wing sizing. The span limitation technically only applies in hover but to increase past the 3 m would require the wings to extend or fold out from the fuselage. Such a reconfiguration method was determined to be at an insufficient technology readiness level. The important factor in *Kwatee*'s wing

TABLE 4.1: Comparison of Basic Sizing Metrics for Analyzed Designs

	Quadrotor	Coaxial Quadrotor	Main Rotor + Quadrotor	Coaxial Main Rotor
Radius	0.625 m (2.05 ft)	0.625 m (2.05 ft)	MR: 1.5m (4.92 ft) Qd: .4m (1.31 ft)	1.5 m (4.92 ft)
Shaft Power	235 kW (175 hp)	212 kW (158 hp)	188 kW (140 hp)	177 kW (132 hp)
DL	1197 N/m <sup>2</sup> (25.0 lb/ft <sup>2</sup> )	1197 N/m <sup>2</sup> (25.0 lb/ft <sup>2</sup> )	795 N/m <sup>2</sup> (16.6 lb/ft <sup>2</sup> )	833 N/m <sup>2</sup> (17.4 lb/ft <sup>2</sup> )
PL	25.1 N/kW (7.58 lb/hp)	27.8 N/kW (8.37 lb/hp)	30.6 N/kW (9.2 lb/hp)	33.3 N/kW (10.1 lb/hp)

design was maximizing the effective wing area while keeping weight low. Details of box wing design is discussed in Chapter 7.

## Blade Design

### 5.1 Design Goals

While the main rotor of a general helicopter is a compromise between hover and edgewise forward flight, *Kwatee*'s coaxial rotor was designed mostly for axial flight. Due to the tailsitter configuration, *Kwatee* primarily operates in either hover in helicopter mode or axial forward flight in fixed-wing mode. This allows for the forward flight conditions to be modeled as a rotor in pure climb. In transition, the rotor blades also maintain axial flight due to the variable incidence box wing and ducted tail fan (see Section 11.2.2). Only in the case of loss of actuation of these systems and in hover with significant side winds would edgewise flight be encountered. This portion of the flight regime is small enough that it was not a key driver for blade design. Each rotor of *Kwatee* employs cyclic and collective controls. The blade geometry (taper, twist, airfoil) was designed to provide high efficiency in hover (FM) and axial flight (propulsive efficiency  $\eta$ ).

### 5.2 Design Methodology

The primary goal of the aerodynamic design of the rotors was to find the rotor geometry that resulted in the best combination of hover (FM) and propulsive efficiency ( $\eta$ ).

$$FM = \frac{C_T^{(3/2)}}{\sqrt{2}(C_{P_i} + C_{P_0})} \quad \eta = \frac{C_T \cdot \lambda_{climb}}{C_{P_i} + C_{P_0}}$$

An in-house large-angle Blade Element Momentum Theory (BEMT) code with table lookup was used to conduct an extensive parametric sweep of different blade geometries (airfoil, taper, twist) as well as optimal RPM for each geometry while MTOW, radius, and solidity were all held constant. The BEMT formulation was adjusted to compensate for the coaxial rotor system. Using momentum theory, the thrust required by each rotor to balance the torque was calculated assuming an induced power interference factor of 1.28 for the lower rotor (56%/44% thrust sharing for upper/lower rotors). This factor takes into account the small inflow velocity the lower rotor experiences due to the wake of the upper rotor.

$$Q_{balance} = \frac{T_U^{3/2} \cdot R}{V_{tip}} = \frac{1.28 * T_L^{3/2} \cdot R}{V_{tip}} \quad W = T_U + T_L$$



The lower rotor was assumed to be completely inside the wake of the upper rotor. The geometries for both rotors were kept the same and the final design is shown in Figure 5.1. *Kwatee's* blade has a 0.1 radius root cut out, an inboard twist of  $-33^\circ/\text{span}$  and an outboard twist of  $-41^\circ/\text{span}$ .

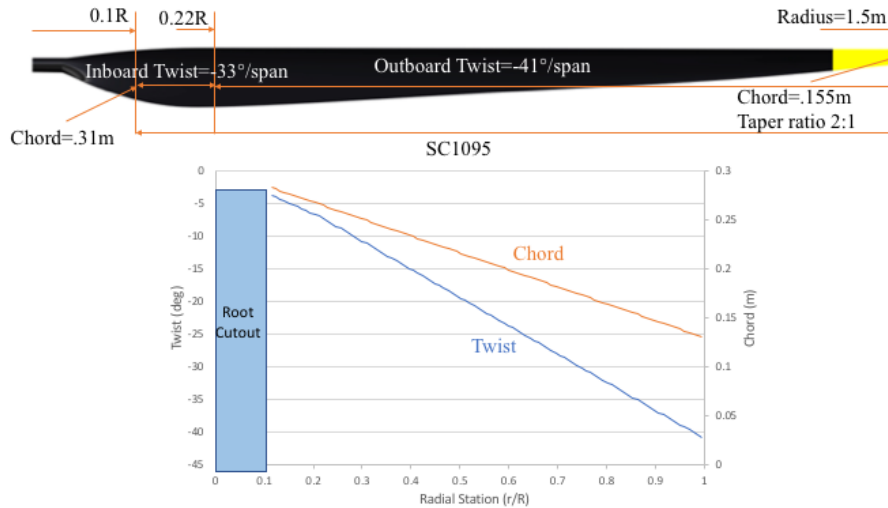


FIGURE 5.1: Geometry of *Kwatee's* Blade Choice

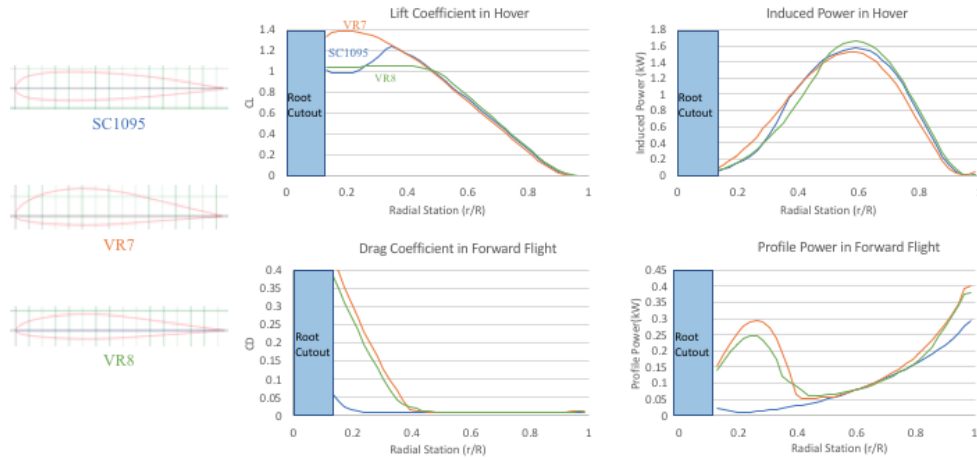
### 5.2.1 Baseline Airfoil Selection

The selection of the rotor airfoil is fundamental to maximizing both hover and propulsive efficiency. When selecting an airfoil, the following aerodynamic characteristics were required: broad range of angle of attack around maximum L/D and around minimum drag coefficient (large drag bucket). The first aerodynamic characteristic is important for a high FM which is mostly governed by induced power coefficient ( $C_{P_i}$ ) for constant thrust. The second aerodynamic characteristic corresponds to profile power coefficient ( $C_{P_0}$ ) and is the main driver of propulsive efficiency ( $\eta$ ).

A total of four airfoils were analyzed: NACA0012, SC1095, VR7 and VR8. The airfoil tables used contained  $C_l$  and  $C_d$  variation with respect to angle of attack and Mach number. The VR7 airfoil has a much higher L/D ratio than the other airfoils as well as a wide range of angle of attacks at max L/D; however, the VR7 has steep  $C_d$  versus angle of attack curve. For hover, the VR7 has good characteristics but the large  $C_d$  values cause a steep increase in  $C_{P_0}$ . This increase in profile drag causes a spike in the overall power thereby lowering propulsive efficiency ( $\eta = 0.49$ ) dramatically. The VR8 airfoil has similar characteristics to the VR7 but does not have as drastic increase of profile power compared to the VR7. This causes the  $C_P$  to be lower for the VR8 but the propulsive efficiency ( $\eta = 0.53$ ) was still too low to be considered for the *Kwatee* airfoil. The SC1095 on the other hand had a much wider drag bucket leading to a much lower profile drag than the VR7 and VR8 as seen by Figure 5.2. The lower profile drag balances out the overall  $C_P$  for the SC1095 allowing for a much higher propulsive efficiency than the VR7 and VR8 ( $\eta = 0.79$ ).

### 5.2.2 Blade Twist and Taper

Incorporation of blade twist and taper can improve the blade hover and propulsive efficiencies. Blade twist affects the inflow distribution on the rotor disk, which can be used to achieve the ideal uniform distribution. On the other hand, blade taper reduces the profile power by enabling the airfoil sections to

FIGURE 5.2: *Kwatee's* Airfoil Comparison in Hover and Forward Flight

operate at the angle of attack for best performance. Due to two different flight regimes, *Kwatee's* blade is a compromise between the best parameters for hover and for forward flight. The parameter sweeps include taper ratio (1 to 3), inboard twist rate ( $0^\circ/\text{span}$  to  $-70^\circ/\text{span}$ ), outboard twist rate ( $0^\circ/\text{m}$  to  $-50^\circ/\text{span}$ ), and tip speed (210 m/s to 240 m/s). This sweep resulted in 7,700 blade designs for each airfoil.

Table 5.1 shows the different combinations of twist rate, and taper that gave the best compromise between FM and  $\eta$ . The chosen blade has an unusual bi-linear twist that slightly lowers the FM but increases the propulsive efficiency. The different flight regimes require a change in root collective from  $40^\circ$  ( $\theta_{75} = 9.2^\circ$  hover) to  $73^\circ$  ( $\theta_{75} = 42^\circ$  forward flight). This collective change is accomplished using individual collective actuators for each rotor blade as discussed in Coaxial Rotor Hub fold out.

TABLE 5.1: Comparison of Basic Sizing Metrics for Analyzed Designs

Geometry	No Taper No Twist Single Airfoil	Linear Taper Linear Twist Single Airfoil	Linear Taper Bi-Linear Twist Single Airfoil
Inboard Twist	$0^\circ$	$-40^\circ$	$-33^\circ$
Transition	0	0	0.2 (r/R)
Outboard Twist	$0^\circ$	$-40^\circ$	$-40^\circ$
Taper	1	2	2
Hover Tip Speed	210 m/s	210 m/s	210 m/s
Airfoil	SC1095	SC1095	SC1095
Figure of Merit	0.72	0.78 (+8.3%)	0.78 (-0.51%)
Propulsive Efficiency	0.23	0.76 (+230%)	0.79 (+3.8%)

The RPM is reduced to 85% of engine continuous power in forward flight. The 85% allows *Kwatee's* engine to still operate around peak efficiency as seen in Section 6.1 but lowers the power applied to the blades. *Kwatee* is expected to spend the majority of mission time in axial flight so the increase in propulsive efficiency was more desirable than the slight decrease in FM. Bi-linear twist also adds some manufacturing complexity to the blade design but the increase in  $\eta$  was deemed worth the extra manufacturing costs. Figure 5.3 shows the progression and efficiency increase as different features were added to *Kwatee's* blades.

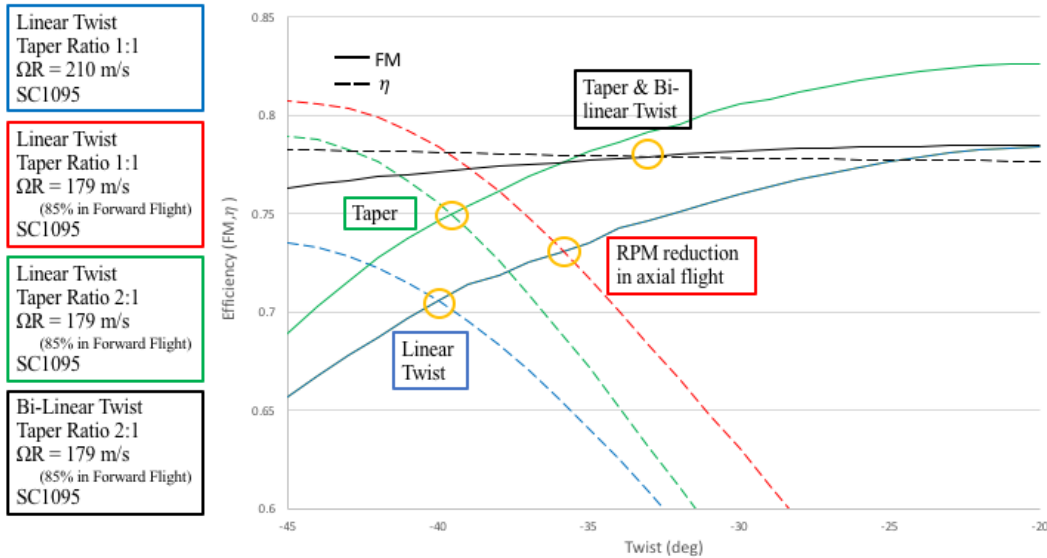


FIGURE 5.3: Progression of Twist and Taper Analysis

### 5.3 Rotor Blade Structural design

*Kwatee* uses a hingeless rotor whose blades are designed to achieve the required strength and stiffness during the different flight profiles. The blades have to withstand centrifugal loads, steady and oscillatory flap, lead-lag and torsional moments, and shear stresses that result from the aerodynamic and inertial forces. The internal structure of the blade was designed to achieve appropriate flap bending, lead-lag bending, torsion bending and axial stiffness. A diagram of the cross-section is seen in Figure 5.4.

The main load-bearing structure of the blades is the D spar made from unidirectional graphite-epoxy that extends from  $0.02c$  to  $0.42c$  from the leading edge. Carbon fiber was chosen over aluminum because of its higher specific strength, better fatigue characteristics and to simplify the construction since most of the vehicle was made from carbon fiber as well. A  $\pm 45^\circ$  carbon fiber composite layup was chosen for the skin to provide adequate torsional stiffness. Nomex Honeycomb was used in the aft section of the cross-section to preserve the aerodynamic profile of the blades.

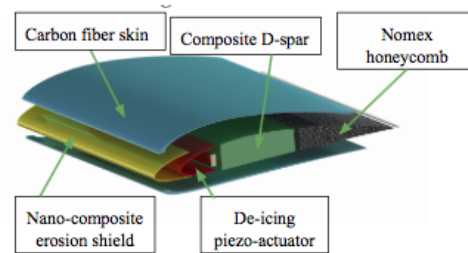


FIGURE 5.4: Rotor Blade Cross Section

A nano-composite erosion protection shield is also used to protect the integrity of the blade components. Custom sized 3M Polyurethane protective tape 8545 was chosen because of its low weight, ease of repair and it offers excellent moisture protection [2]. *Kwatee* has the ability to operate at high altitudes where it can be exposed to very low temperatures. Therefore, a non-thermal based de-icing system is used since it consumes less energy than conventional electro-thermal based methods. The de-icing system consists of a series of actuators located between the blade skin and the erosion shield layer that produce high frequency vibration to break any ice particles that might have accumulated on the blades [3]. The centrifugal forces then cause the ice to break off the surface of the skin.

## 5.4 Hub Design

The Coaxial Rotor Hub fold-out shows the details of *Kwatee* hub. A concern when designing the hub was blade impact that can occur due to the lack of stiffness in the flap direction. Since *Kwatee* might have more significant edgewise flight during transition if either the variable incidence box wing or ducted fan cannot be actuated, an articulated hub would lead to blade interference which immediately eliminated it as a possibility. The fan plots in Figure 5.5 were calculated for two different flight conditions: hover (a) and axial forward flight (b) because the RPM and collective pitch values are different. Because it is a coaxial rotor, both blades were designed to flap stiffness that ensured no blade strikes in all flight conditions. In both conditions, the first flap frequency was designed to be 1.53/rev.

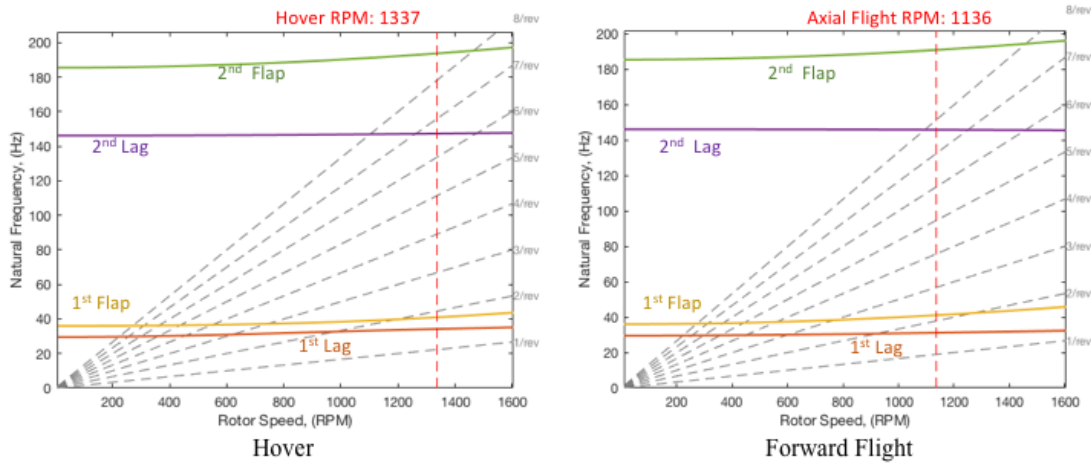


FIGURE 5.5: Fan Plots for Hover (a) and Axial Flight (b)

### 5.4.1 Blade Grip Design

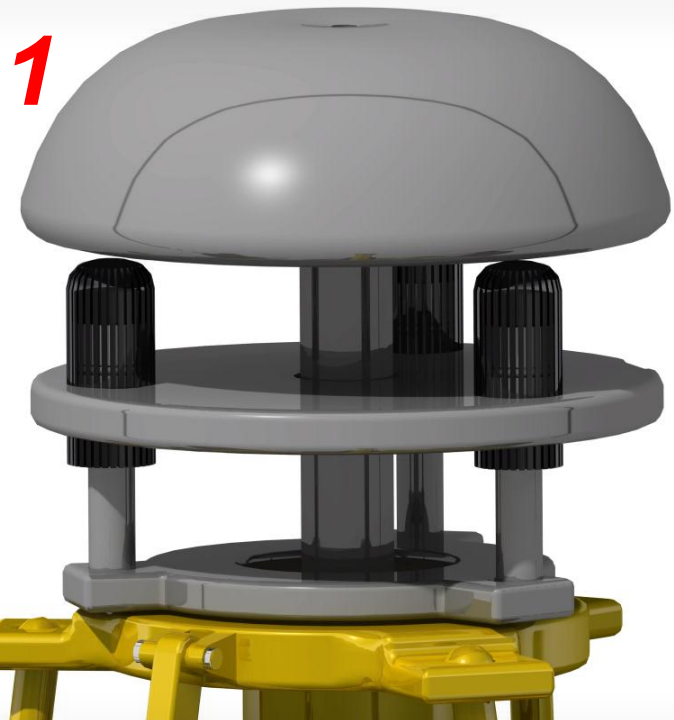
When analyzing possible blade grip designs for *Kwatee*, there were three criteria: (1) Simple, (2) allow for circular blade root for a clean fit with the spinner, and (3) Rigid. Upon reviewing multiple styles of rigid blade grips, a Patent submitted by Gupta and Karem [4] describing a method for connecting a composite blade was selected.

A composite blade is attached to this grip by taking advantage of the centrifugal forces the blade undergoes while in use. The rotor is designed in such a way that the the most inboard section of the root is larger in diameter than that of the outboard section of the root. The blade grip is a sleeve that fits over the blade root and due to the taper, does not allow the blade to move. An image of the grip can be seen on the Coaxial Rotor Hub fold out.

This design met all of the criteria set forth and was easily implemented into the hub design. The simple construction means easier maintenance and a lower chance of failure. The blade strength is also improved with this design over traditional attachments, due to using centrifugal forces instead of the traditional bolt style attachment.

# Coaxial Rotor Hub Design

Six independently controlled actuators allow for full cyclic and collective control of each rotor set.



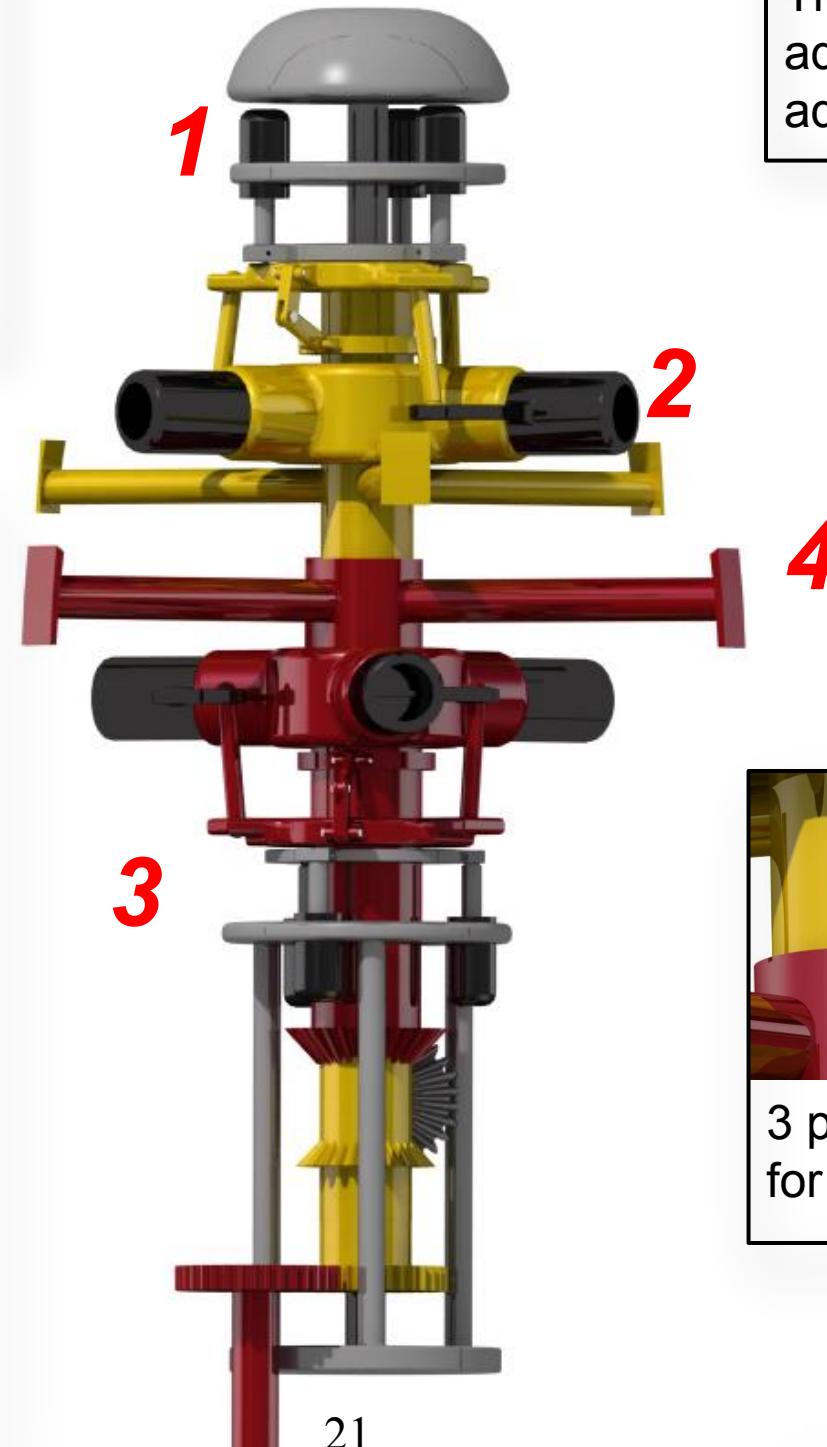
Rotates CW

Rotates CCW

Stationary

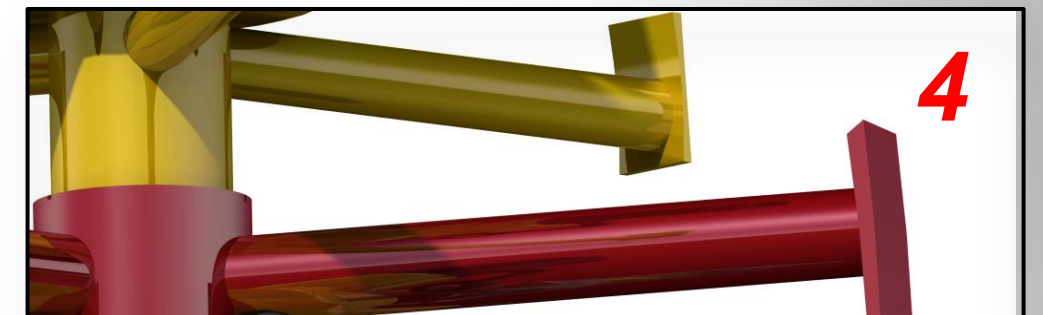
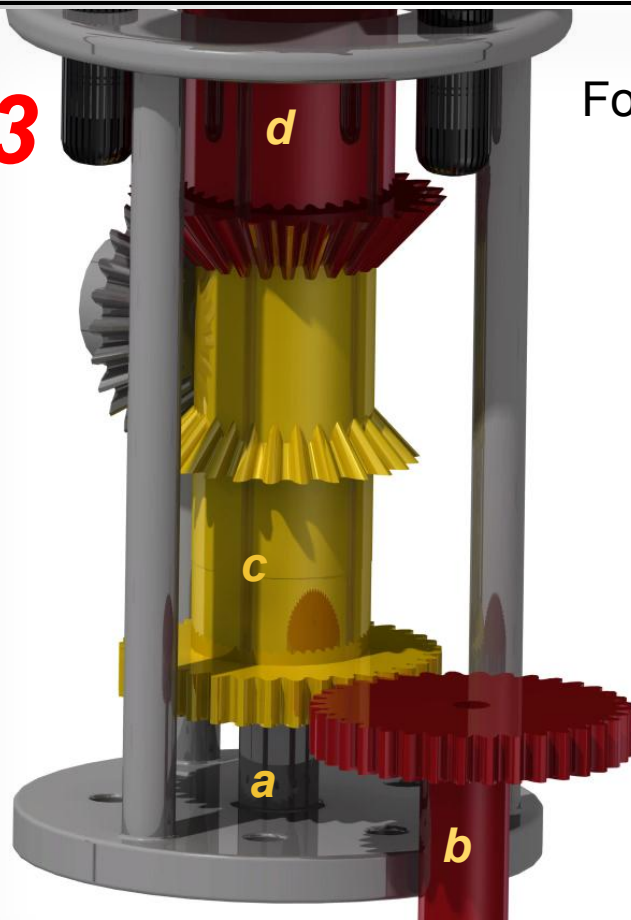


The blade grips for this hub design take advantage of centrifugal forces and advancement in composite blades



3

Four main shafts:  
 (a) Structural shaft  
 (b) Input shaft  
 (c) CW rotor shaft  
 (d) CCW rotor shaft



3 post on each of the rotating shafts allow for solid attachment points to the spinners.

# Power System Overview

Based on the RFP and mission requirements, *Kwatee* is designed with an installed power of 194 kW (260 hp). A twin turboshaft setup using Stuttgart Engineering STV130 engines with direct mechanical coupling was chosen to drive the rotor system and provide auxiliary power [5]. The engines are mounted within the fuselage near the base of the rotor system, and power the rotor through a gearbox and sprag clutch. A combination auxiliary power unit (APU) and alternator supply small amounts of engine power to feed the avionics and controls systems.

## 6.1 Powerplant Selection

A trade study of over 12 commercially available powerplants was performed for a baseline comparison of different types of engines. RFP requirements emphasize high speed forward flight and efficient hover. An ideal engine would have high specific power and low specific fuel consumption (Sfc) at the levels of power required for *Kwatee*'s missions.

The four types of engines specifically examined in the trade study include gasoline piston engines, diesel piston engines, rotary (Wankel) engines, and turboshaft engines (Table 6.1).

TABLE 6.1: Comparison of Engine Types for Powerplant Selection

Engine Type	Specific Power	Sfc	Relative Advantages	Relative Drawbacks
Gasoline Piston	moderate	moderate	Reliability, ease of service, low cost	Average performance characteristics
Diesel Piston	low	low	Excellent efficiency, reliability	High powerplant weight
Wankel	high	high	Lightweight, compact	High maintenance, poor efficiency
Turboshaft	high	high	Very lightweight, compact	Poor efficiency

As seen in Figure 6.1, diesel piston engines have low Sfc but low specific power. Compared to the diesel engines, turboshaft engines have specific power figures of over 3.0 kW/kg (1.85 hp/lb) but Sfc's of approximately 0.19 kg/kWh (0.55 lb/hphr). A turboshaft engine was chosen over a single KM503d rotary engine due to the superior specific power of the typical turboshaft engine. A comparison of the simulated total powerplant system weights (including engine, fuel weight, fuel system) showed that the total weight of a turboshaft system was lower than that of a diesel system for all missions under 1.8 hours flight time.



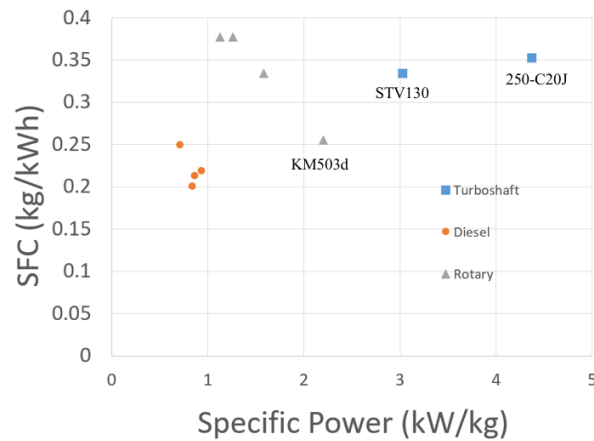


FIGURE 6.1: Specific Power vs. Fuel Consumption for Possible Engines

### 6.1.1 Engine Operation

The two contenders for a turboshaft engine system were the Stuttgart STV130 and a Rolls Royce 250-C20J. At 3,000 m operating altitude, where most flights will occur, both engines have a specific power of 3.05 kW/kg (1.86 hp/lb), but the STV130's lower Sfc will allow for lower overall weight and longer operating range. Additionally, a twin STV130 setup does not require the 'rubber' engine design process, provides redundancy in case of engine failure, and allows for more efficient operation during low power flight (cruise). Both engines are operated at near full power (where turboshaft engines are most efficient) during hover and dash. During lower power flight regimes, one engine can run at idle while the other provides power at its optimal Sfc level. Using this power distribution method, the propulsion system may be tuned to provide optimal Sfc during all flight regimes.

### 6.1.2 Transmission

To transmit the power from the engines to each rotor blade, a mechanical linkage was designed to meet *Kwatee's* specific requirements. The transmission allows for two inputs from the engines with a single output shaft. From the input reduction transmission, a shaft drives one set of rotors. Attached to this shaft is a system of bevel gears that allow for a complete torque reversal that supplies the counter rotating shaft. A diagram of this is included on the Coaxial Rotor Hub fold-out.

## 6.2 Cooling System

The twin turboshaft system does not require a traditional liquid loop radiator unlike piston internal combustion engines. Instead, engine temperatures are closely monitored and controlled by a full authority digital engine control (FADEC) system by balancing fuel burn, power output, and ambient temperature and density. The engine gearboxes have self contained oil cooling radiators, which are cooled by a part of the air entering the air intakes (Figure 6.2).

## 6.3 Lubrication System

The lubrication system in *Kwatee* is of particular importance due to both vertical and horizontal flight regimes. Oil quality and circulation must be carefully managed in both orientations to ensure safe and dependable operation.

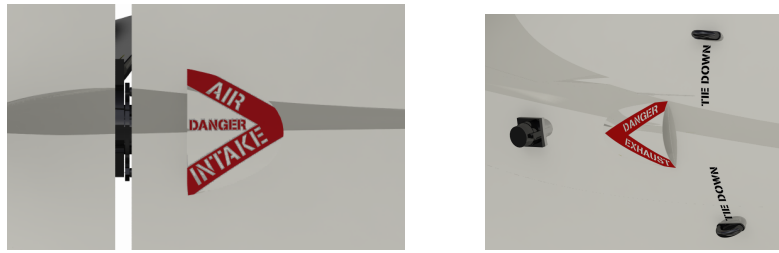


FIGURE 6.2: Engine Intake and Exhaust

A dry sump lubrication system was chosen for its adaptability to flight orientation and inertial forces. A dry sump system utilizes multiple pumps and filters to prevent oil starvation or oil flooding of critical engine components. Dry sump pumps draw oil from the engine to cool and store in a separate reservoir after being filtered of particles or excess air. Fresh oil is then directed to the engine with additional pumps. The pressurized oil is directed using pumps, and is not affected by changes in orientation or aggressive flight maneuvers.

## Wing Design

*Kwatee* utilizes a novel closed-loop box wing design to maximize wing area and lift efficiency in the geometric constraint provided by the RFP and operation in megacity environment. The wing has a total planform area of  $4.1 \text{ m}^2$  ( $44.1 \text{ ft}^2$ ). This section will detail the design considerations for choosing a box wing and selection of airfoil sections, taper, stagger, and gap.

### 7.1 Box Wing Selection

The limited span is the driving factor for choosing a box wing. A mono wing design can be lighter with lower profile drag. Because of the 3m span restriction, the resulting low aspect ratio would lead to very poor lift efficiency. A high wing loading would also lead to poor low speed stability and undesirable stall characteristics. A biplane design mitigates many of these issues, at the cost of increased weight and profile drag. To address these issues, a box wing was considered. This novel wing design greatly reduces induced drag, and increases structural rigidity by connecting upper and lower wingtips with box wing sides.

A traditional monoplane or biplane design has span efficiency factor  $e < 1.0$ . In comparison, a rectangular box wing has a span efficiency factor of 1.46 [6]. Stagger and gap were chosen to maximize aerodynamic benefits of each while keeping a compact size. A stagger and gap of 1.3 times the mean chord length were chosen (1.0 m).

### 7.2 Airfoil Selection

A study of a range of available airfoils was performed to give *Kwatee* efficient forward flight and controllable low speed and stall performance. *Kwatee's* missions focus on steady forward flight and transitions between horizontal and vertical flight, with limited high-g maneuvers. As a result, the wings and airfoils were sized to generate 600kg of lift, the MTOW of the vehicle.

The Wortmann FX 63-137 airfoil was chosen as the airfoil for the *Kwatee* wing. Of the airfoils analyzed, the FX 63-137 has a high L/D, and minimal loss of lift as the airfoil approaches stall. When fully loaded, *Kwatee's* operating angle of attack ( $\alpha$ ) range is  $-6^\circ$  at max dash (3,000 m) to  $10^\circ$  at stall (SLS). The

airfoil maintains an  $\alpha$  of  $-2^\circ$  at a 277 km/h (150 kts) cruise (3,000 m). The airfoil stalls at  $10^\circ$  and an airspeed of 144 km/h (78 knots) (Figure 7.1).

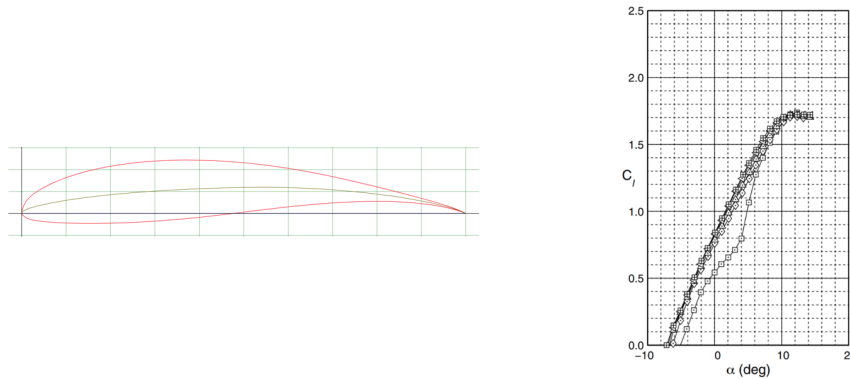


FIGURE 7.1: Wing Airfoil and Profile Lift vs Angle of Attack Characteristics

The variable incidence box wing mechanism is used to vary the pitch setting of the wing at the desired  $\alpha$  while keeping the fuselage horizontal, reducing profile drag. During transition, the tilting mechanism will also allow the fuselage to be oriented properly; thereby, maintaining the wings at an incidence below the stall angle of  $10^\circ$ .

### 7.3 Taper Ratio

The wing taper ratio was chosen to reduce structural loads at the root, blend the wingtips into the box wing sides, and increase efficiency during high speed flight. A 2:1 ratio was chosen, with root chord ( $c_{root}$ ) of 1.0 m (3.3 ft) and tip chord ( $c_{tip}$ ) of 0.55 m (1.8 ft). The upper wing gently slopes downwards, and lower wing upwards, to blend into the vertical box wing sides. The box wing sides have a NACA 0012 profile with  $c = 0.2$  m (0.65 ft). The final wing design characteristics are listed in table 7.1.

## 7.4 Wing Structural Design

*Kwatee's* wing is optimized for high bending stiffness needed during forward flight. The construction of the wing is simple as shown in Figure 7.2 - it is composed a of torque box, whose front vertical web is located at  $0.1c$  and the rear web at  $0.45c$ . The thickness of the front and rear webs is 8.5 mm (0.335 in.) while the top and bottom layers have a thickness of 5.5 mm (0.217 in.) The lay up for the top and bottom skin webs is  $[\pm 45^\circ]$  orientation of plies, each 0.127 mm (0.005 in.) thick. The other structural components of the wing include the ribs and skin that improve the wing's stiffness and aid with load transfer during flight. The hinge of the upper wing attaches to the fuselage at a bulkhead and was designed to allow for the change of incidence angle while maintaining structural integrity. The lay up for the front and rear webs is  $[0_9/90_9/\pm 45]_S$ . The skin consisted of angular and cross plies of graphite-epoxy, designed to provide torsional stiffness to the wing.

### 7.4.1 Material Selection

From a structural standpoint, an efficient wing is one that is capable of withstanding all the loads it is expected to be subjected to during service while also being as lightweight as possible. When deciding upon the material to be used to manufacture the wing, the density and hence the weight of the different materials were considered. Graphite-epoxy composite material, while more expensive than was

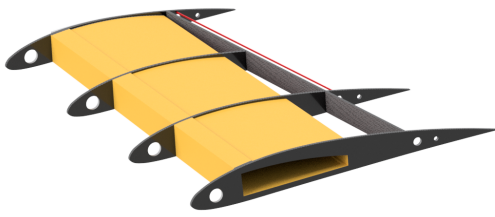


FIGURE 7.2: Cross section of the wing

TABLE 7.1: Wing Geometry

Wing Geometry	Value (SI)
Aspect Ratio (Upper)	3.23
Aspect Ratio (Lower)	4
Wing Area	4.1 m <sup>2</sup> (44.1 ft <sup>2</sup> )
Operating $\alpha$	-6° to 10°
Airfoil Shape	Wortmann FX 63-137
Stall Speed	144 km/h (78 knots)

chosen for the construction of the ribs and spars because it met the material stiffness requirements of the design while providing reduction in weight, thereby significantly reducing the empty weight of the aircraft.

Because the wing is made of composite materials, it can be constructed as a single long continuous unit. Unlike conventional curing methods using an autoclave, out-of-autoclave (OOA) techniques such as Vacuum Assisted Resin Transfer Molding (VARTM) reduce the cost and complexity of manufacturing large scale composite parts while maintaining product quality. Given that composite materials are poor conductors of electricity, a copper mesh is applied to the outer-most ply of the wing to prevent damage to the structure in the event of a lightning strike. Static discharge wicks are attached to the trailing edge of the wing to prevent build up of static charges. Because *Kwatee* can fly at high altitudes, it is necessary that some form of de-icing be incorporated into the wing. A thermal-based anti-icing system was chosen over alternative de-icing mechanisms to ensure that no ice forms along the wings leading edge.

## Performance Analysis

### 8.1 Hover Performance

Final hover power requirements were calculated using the in-house BEMT code discussed Section 5. Hover performance varies at different altitudes due to the difference in density. Table 8.1 shows the hover time available with a 50% fuel burn using the metrics from the Stuttgart STV130 engines discussed in Section 6.1.

TABLE 8.1: *Kwatee's* Hover Time with 50% Fuel Burn

Altitude	Hover Time
Sea Level	1.74 hr
3000 m	1.45 hr

### 8.2 Drag Estimation

Drag estimation is important for calculating maximum speed and range during forward flight. Drag was broken down into three components: parasitic drag, profile drag, and induced drag. Parasitic and profile drag of the vehicle were combined into one value, while induced drag of the wings was calculated as a function of lift coefficient.

An equivalent flat plate drag area was calculated using a drag buildup method detailed in Kroo [6]. The profile (blades, wings) and parasitic (fuselage struts, air intakes, landing gear) drag component of each main component of the aircraft was calculated using three factors: exposed surface area, form factor, and skin friction coefficient. The estimated exposed surface area was determined using CAD models. The form factor of each component was determined using individual thickness-to-chord and fineness ratios and data given in Kroo [6]. The skin friction coefficient is determined using an approximate Reynolds number and partially turbulent boundary layer.

Table 8.2 shows the breakdown of drag contributions of each component. The total flat plate area was increased by 25% to account for various miscellaneous items on the vehicle such as avionic sensors, payload door latches, control surface gaps, etc - giving a final estimated flat plate area of  $0.156 \text{ m}^2$  ( $1.681 \text{ ft}^2$ ). This figure is used for all forward flight performance calculations.

TABLE 8.2: Breakdown of Drag Contributions

Component	Flat Plate Area ( $m^2$ )	Flat Plate Area ( $ft^2$ )	Percentage
Fuselage	0.038	.409	30.4%
Wings	0.073	0.785	58.4%
Fins	0.011	0.118	8.8%
Strut	0.002	0.022	1.6%
Landing Gear	0.001	0.011	0.8%
Total	0.125	1.345	100%
Add 25% allowance	0.156	1.681	125%

Note the low flat plate area due to the excellent fineness ratio of the fuselage. Overall, the non-lifting surfaces of *Kwatee* generate less than 50% of the total flat plate area.

### 8.3 Forward Flight Performance

Forward flight power requirements were calculated using the equivalent flat plate area, and induced drag of the wings. Flight performance varies at different altitudes, due to differences in dynamic pressure. As shown in Figure 8.1, significantly less power is required at an operating altitude of 3,000 m (10,000 ft) due to decrease in profile drag.

Figure 8.2 shows specific range as a function of the flight speed. The velocity for best range is determined to be 263 km/h (142 knots) at the maximum value on the 3000 m curve (shown in blue). The velocity for best endurance occurs at a minimum power required of 56 kW (75 hp) and 180 km/h (95 knots) at sea level and 65 kW (87 hp) and 205 km/h (110 knots) at 3,000 m.

With a maximum power output of 194 kW (260 hp) from the twin STV130 propulsion system, *Kwatee* is power limited to 389 km/h (210 knots) at sea level, and 425 km/h (230 knots) at 3,000 m. Lower dynamic pressure at high operating altitude significantly reduces profile drag, especially at high speeds. Max range and dash speeds are achieved at 3,000 m altitude.

*Kwatee* has a nominal fuel capacity of 100 kg (220 lb) when carrying a 100 kg payload. Various mission fuel and payload configurations are possible to prioritize operating range or carry extra payload for short range missions, shown in Table 8.3. Max payload size may be prioritized at the cost of lower fuel weight and consequently lower range, and vice versa.



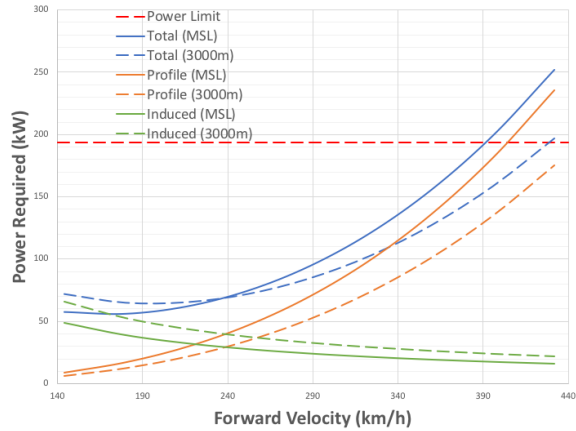


FIGURE 8.1: Power Required vs. Axial Velocity

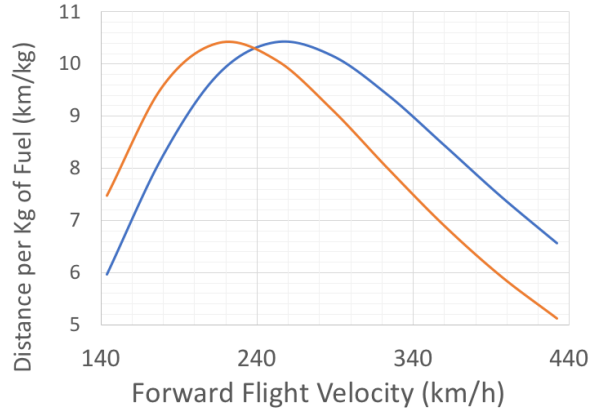


FIGURE 8.2: Distance per kg Fuel vs. Axial Velocity

TABLE 8.3: Summary of Forward Flight Performance Metrics (100kg fuel)

Maximum Range (50% fuel capacity)	515 km (278 NM)	263 km/h (142 knots)
Maximum Endurance (50% fuel capacity)	2.73 hours	176 km/h (95 knots)
Maximum Dash Speed (3,000 m altitude)	-	425 km/h (230 knots)

# Airframe Structural Design

*Kwatee's* airframe has been designed to be structurally robust and aerodynamically streamlined to enable efficient high-speed operation. With the space requirement of the RFP, a balancing of the cargo capacity, weight, strength and drag penalties resulted in a design that has a fineness ratio of 5. The aircraft structure is semi-monocoque design that is composed of a load bearing skin and a framework of bulkheads, longerons and stringers. Figure 9.1 shows the layout of the four sections of the fuselage.

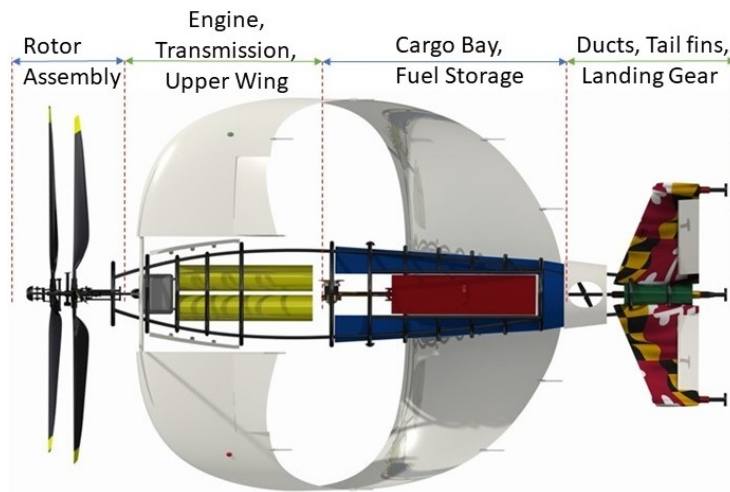


FIGURE 9.1: The four main sections of *Kwatee*

The front of the aircraft consists of the rotor hub assembly covered by spinners, followed by the wing attachment, transmission and engine. The third section has the payload and fuel tanks while the last section has the ducts, vertical fins and landing gear. All of the vehicle's components were positioned to achieve short load paths and minimize the displacement of the center of gravity during transition and flight.

## 9.1 Load Paths

*Kwatee* is exposed to different loads during the three operations – when on ground, in hover and during forward flight. The internal structure has been designed to enable a smooth transfer of these loads to the airframe where these loads are dissipated.

In forward flight, the main load is from the lift produced by the wings that is carried by the torque box. All loads on the torque box are disseminated into the fuselage via the wing box that is attached to the bulkheads. The weights of the engine, fuel and payload, are supported by the bulkheads. There is a separate bulkhead at the point where the strut from the lower wing is attached to the fuselage that dissipates the lift forces from the lower wing. The load paths are shown in Figure 9.2. The green arrows represent the lift forces, yellow arrow represents the weight of the engine assembly, blue arrows represent the weight of the payload and fuel, and the orange arrows represent the weight of the duct assembly in the rear part of the vehicle.

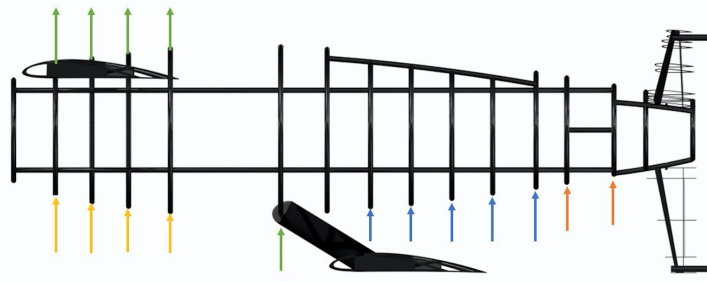


FIGURE 9.2: Load paths during forward flight

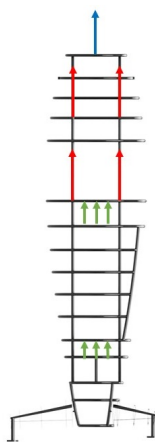


FIGURE 9.3: Load paths during hover

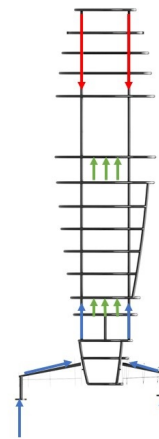


FIGURE 9.4: Load paths on ground

During hover, the primary loads are thrust force from the rotor and weights of vehicle components, payload and fuel. Figure 9.3 shows the thrust force represented by the blue arrow and load paths shown by the red and green arrows. During ground operations, the load path is distributed evenly between the landing gear positioned on the tips of the three tail surfaces. The load is transferred to two angled vertical spars in the tail structure that transfer loads directly to longerons in the fuselage. Overall, there is a smooth and direct load path represented by the blue arrows in Figure 9.4 from each landing gear to the fuselage where the force is then dispersed. Secondary loads include the weights of the engine, payload and fuel. The green arrows represent the weights of the vehicle components supported by the solid bulkheads while the red arrows represent the weight of the rotors dispersed by the longerons.

## 9.2 Fuselage Structure

*Kwatee* has a semi-monocoque fuselage. Its airframe consist of strategically placed bulkheads, longerons and stringers to carry loads throughout the fuselage. Primary bulkheads are located between each of the four sections shown in Figure 9.1 and at points of attachments of wings and fins.

All the bulkheads utilize a simple I-beam profile to support radial loads [7]. The first set of the primary bulkheads are at the end of the rotor hub. The engine bay consists of two primary bulkheads at each end, and a set of strategically placed half bulkheads that constrict the movement of the engine to save on weight. The half bulkheads were chosen over one solid bulkhead to save on weight while achieving the same role of constricting the engine movements. Half-bulkheads are also used in the pay-load bay for similar reasons. Two secondary bulkheads can also be found in each end of the duct assembly. Two more bulkheads are in the far most part of the fuselage. They provide attachment points for the angled spars that run across the tail fins and support the vertical forces produced by the fins during forward flight. The engine bay and payload doors also consist of bulkhead continuations to ensure a smooth transfer of loads. Additional longitudinal and vertical supports create a door frame around the opening of the cargo bay door.

The longitudinal beams need to resist bending in forward flight and axial loads during hover and when on the ground. Therefore, they utilize a top hat beam profile for its inherent bending strength along both longitudinal and vertical axes. Four primary longitudinal beams run along the fuselage and support all the longitudinal loads in hover and when the vehicle is on the ground. The Internal Structure fold-out shows a detailed layout of internal supports.

## 9.3 Lower Wing Strut

A NACA 0012 symmetric strut is used to attach the lower wing to a bulkhead in the fuselage for load transmission as shown in Figure 9.5. The strut is made from carbon fiber. Inside of the strut is a linear actuator that is pinned on both sides. The actuator is the driving mechanism that allows *Kwatee* to vary the angle of attack of the box wing. To accommodate the rotation of the strut about the bulk head, a slit in the fuselage as well as the wing, is incorporated as seen in Figure 9.5.

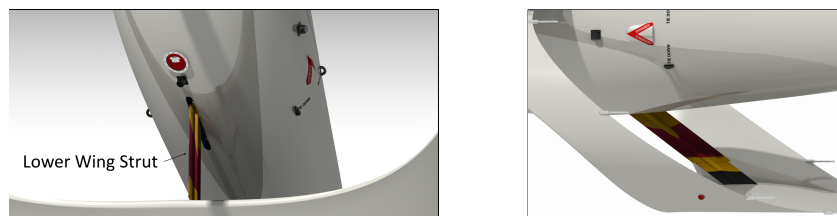


FIGURE 9.5: A strut attaching the lower wing to the fuselage



## 9.4 Hard Points

To make vehicle storage easy and safe for the customer *Kwatee* includes four hard points (Figure 9.6) that attach directly to a bulkhead of the internal frame. Upon the completion of flight operations, tie downs can be attached from these hard points to anchor points on the ground. This allows for easy storage and transportation of *Kwatee* and also prevents the vehicle from toppling over in strong gusts.



FIGURE 9.6: Tie down attachment points

## 9.5 Rotating Shroud

*Kwatee* includes a ducted tail fan to aid in transition maneuvers. While in forward flight, however, the fan creates unnecessary drag. To clean up the design aerodynamically, a simple mechanical system is included to rotate a shroud that completely seals off the duct while in axial flight (Figure 9.7). The inside of the rotating shroud includes a track that allows for an electric motor driven gear to rotate the sleeve about the aircraft center line.



FIGURE 9.7: Rotating shroud that covers up the ducts during axial flight

## 9.6 Tail Fin

*Kwatee* consists of three tail fins. The internal structure of these fins consist of two angled spars and ribs as shown in Figure 9.8. The leading edge spar provides attachment of the landing gear (Figure 9.9) and transmits the landing loads smoothly to the longerons. The two spars are also attached to separate bulkheads in the fuselage that carry the vertical forces generated by the fins while in forward flight.

## 9.7 Landing Gear

*Kwatee* has three oleo-pneumatic landing gear. Retraction of the landing gear was considered but decided against because it added structural complexity and weight, and also because there was insufficient volume for retraction. Instead, the landing gear are faired to maintain a smooth aerodynamic profile to minimize profile drag during forward flight. The landing gear are sized for a gross weight of 620 kg (1,366.87 lb.), a dynamic load factor of 2 and a safety factor of 1.5 [8]. The landing gear were sized for multiple landing conditions, which included one gear touching down first, landing on a 15° slope, and three-point vertical landing.

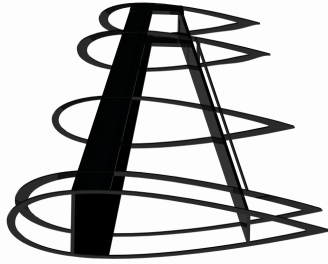


FIGURE 9.8: Internal structure of the tail fin

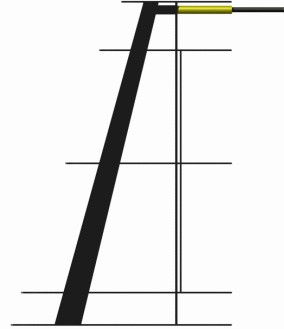


FIGURE 9.9: Landing gear attachment

### 9.7.1 Sealed Oleo – Pneumatic Strut Sizing

Single cantilever oleo-pneumatic shock absorbers are used for all three landing gear [9]. Each landing gear strut was designed for a drop velocity of 10 ft/s. Assuming a load factor of 2.0, energy absorption efficiency of 0.80 [10], the total stroke and diameter of the oleo-pneumatic strut was calculated to be 198 mm (3.9 in.) and 88.9 mm (3.5 in.) respectively. An internal pressure of 12,411 kPa (1,800 psi) was chosen for the oleo to allow for servicing with standard compressors.

## 9.8 Material Selection

*Kwatee* airframe was designed to be strong yet lightweight for maximum efficiency and speed. Several materials including carbon fiber-epoxy, Kevlar, aluminum, titanium and steel were considered for use in fabrication of the aircraft components. Steel was eliminated because of its low strength to weight ratio when compared to aluminum, carbon fiber and Kevlar.

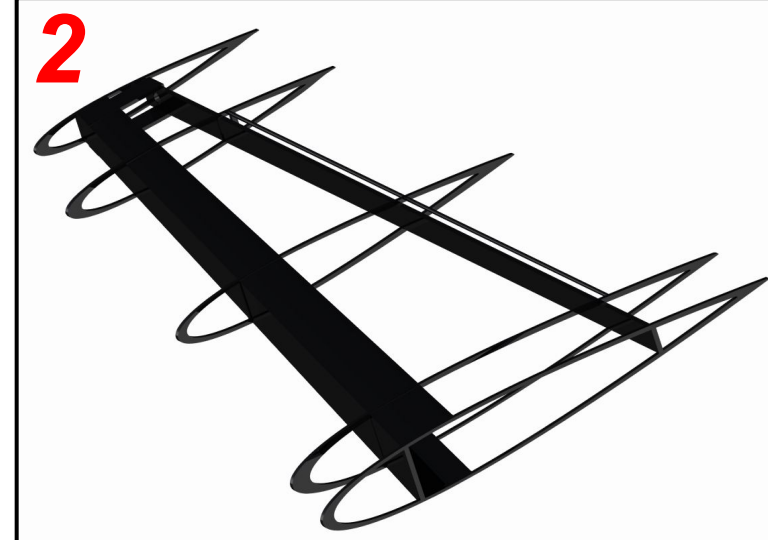
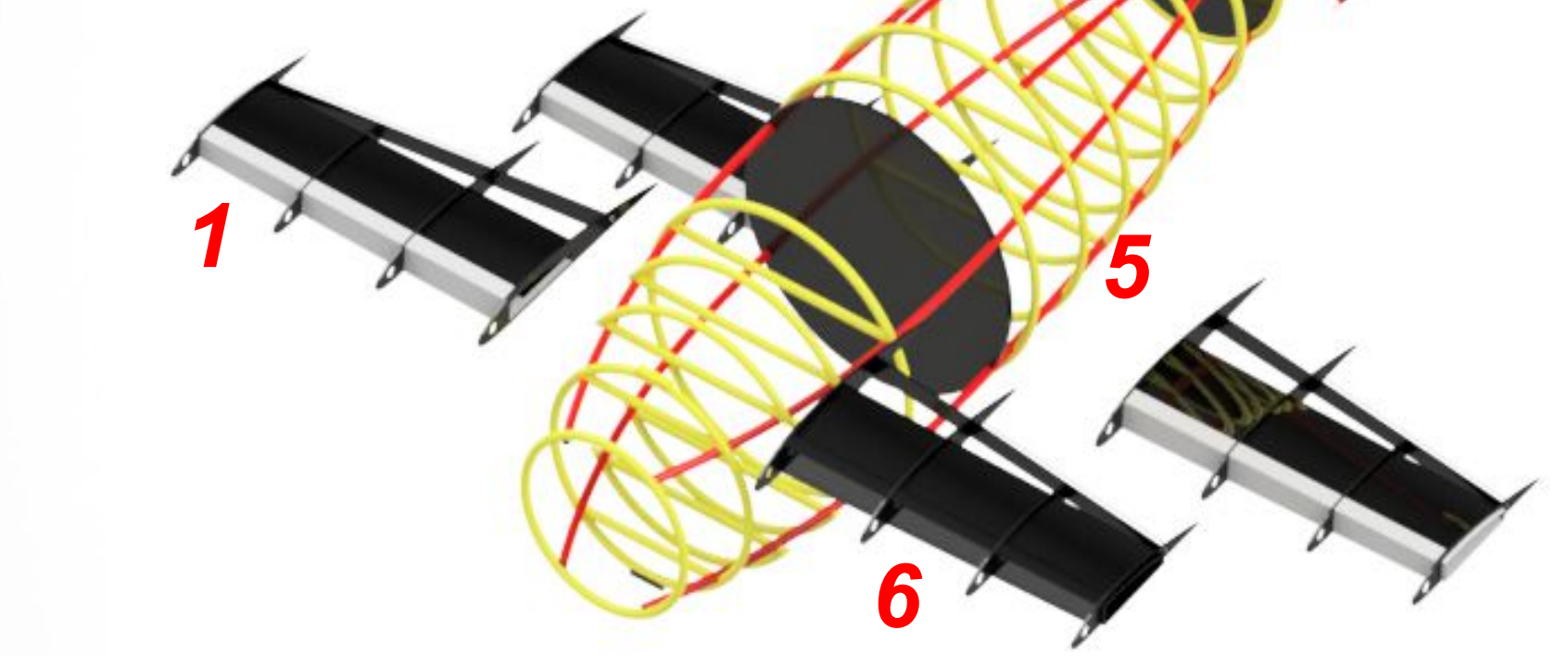
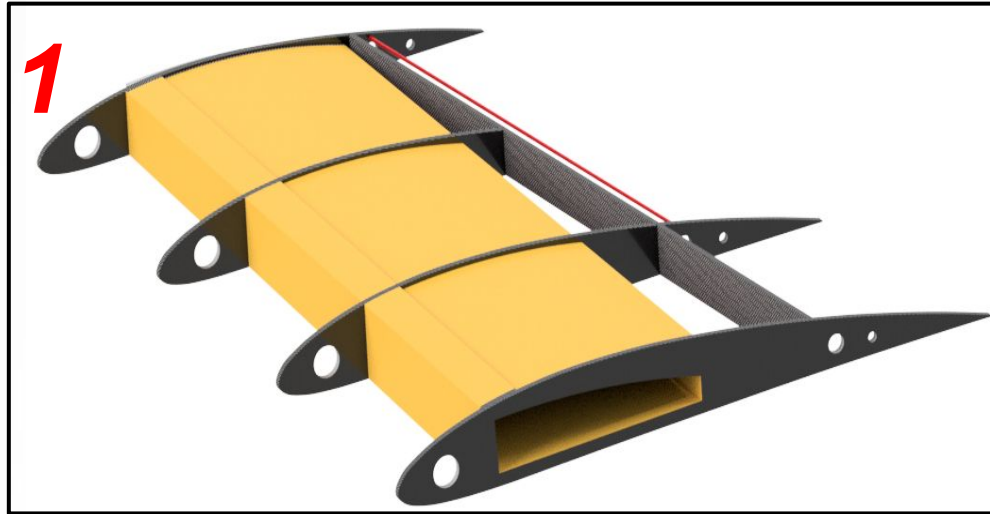
Two materials were considered for the skin – carbon fiber and Kevlar. They are both composites that offer weight savings and simplify the fabrication process. Aluminum and carbon fiber-epoxy were considered for the internal airframe. Aluminum risks galvanic corrosion when in contact with carbon fiber [11]. Therefore, the two options were to either use aluminum for the airframe and Kevlar for the skin, or to use carbon fiber-epoxy for both the airframe and the skin. The latter was chosen for the construction of *Kwatee*.

Carbon fiber-epoxy skin provides a smooth outer surface that is lightweight and has a low skin friction coefficient. The manufacturing of composites using out of autoclave (OOA) pre-pregs allows for manufacturing of large smooth continuous carbon fiber panels that reduce drag interference at panel joints such as rivets. Continuous panels also increase the airframe stiffness and crash-worthiness rating while reducing the number of fasteners and support structures needed to attach the skin to the primary structure. The carbon fiber skin of the fuselage and wings consist of layers of  $\pm 45^\circ$  and  $0/90^\circ$  carbon fiber laminae.

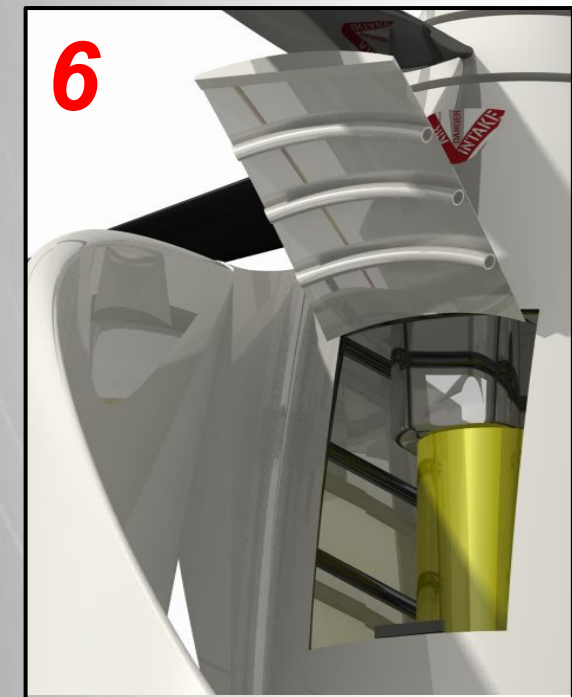
Titanium is used in limited quantities. Its properties of high specific strength, corrosion resistance and high temperature stability are best suited for the engine bulkheads. Ti-3Al-2.5V alloy is used for the landing gear because they offer weight savings compared to steel tubes.

# Kwatee Airframe Internal Structure

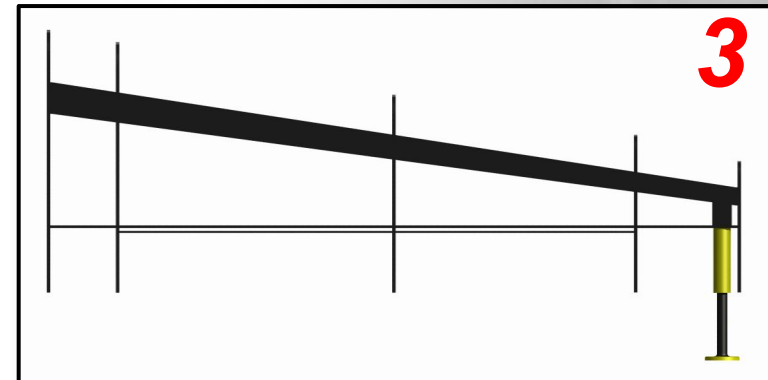
The internal wing structure includes carbon fiber ribs, along with a torque box, and aileron hinges.



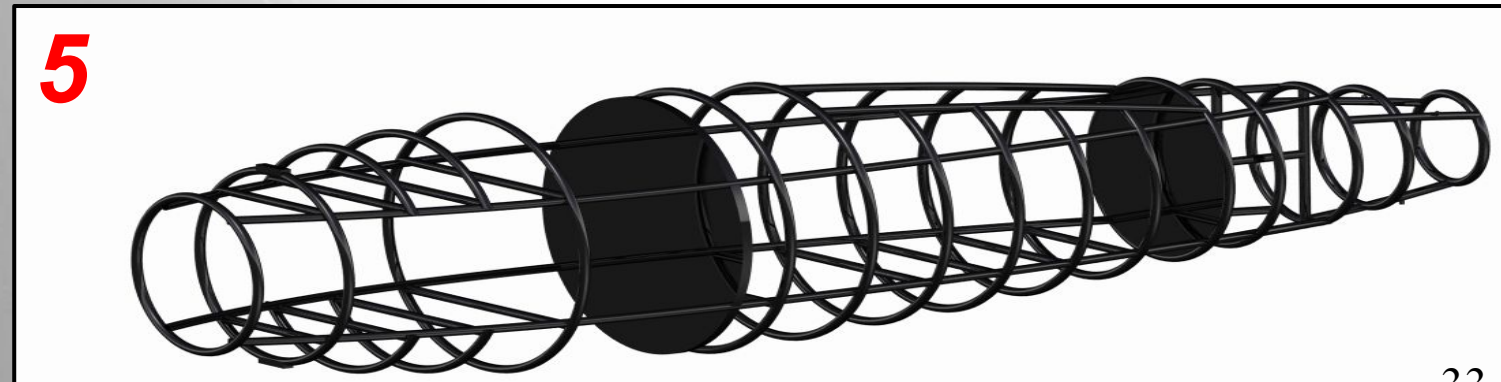
Tail fin structure consists of carbon fiber ribs, rudder hinges, and angled spars with reinforced landing gear attachment point.



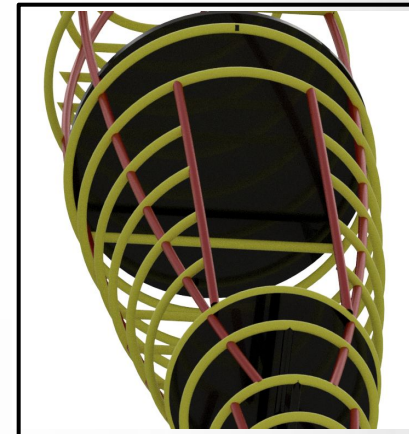
Doors consist of bulkhead continuations for smooth load transfer



The sealed oleo - pneumatic landing gear is attached to the angled spar



The main airframe consists of carbon fiber bulkheads, longerons and stringers. Half bulkheads are used for engine and payload placement, and door frames are created for the payload door.



Door frame ensures structural integrity of the fuselage

## 9.9 Mitigation of Lightning and Static Charges

*Kwatee's* skin is carbon fiber epoxy composite, which builds up static charges during flight. This can be hazardous during ground operations such as loading and unloading the payload, inspection and performing maintenance on the aircraft. To prevent this, a copper mesh is placed on the skin to eliminate the risk of galvanized corrosion that occurs when in contact with carbon composites. The wings are also equipped with static discharge wicks that prevent the build up of static charges in flight.

# Avionics

## 10.1 Mission Requirements

*Kwatee's* avionics and sensors suite has been designed to provide full autonomy for the complete range of its missions. The avionics suite incorporates the latest in proven and commercially available technology to obtain the best performance out of the aircraft while minimizing size, weight and power requirements. The payload deployment mission uses a fully autonomous system and autopilot technology capable of unmanned flight through the entire span of flight. *Kwatee's* avionics suite is also versatile in nature such that, if necessary, the sensors would be capable of performing various other missions in addition to disaster relief, such as surveillance or telecommunication. The various requirements for unmanned flight that lead to the choice of *Kwatee's* avionics are as follows:

- **Flight:** An integrated IMU and flight controller take the responsibility of inputting inertial measurements and sensor readings and outputting data to the flight actuators and control surfaces using software control algorithms. This allows the aircraft to function entirely independent of human interaction. Here, feedback control, sensor fusion, collision avoidance algorithms, and health and usage monitoring systems are all processed. In addition, *Kwatee* utilizes pressure, pitot-static and temperature sensors to obtain necessary flight and velocity data.
  - **Collision Avoidance:** To obtain full autonomy, *Kwatee* must be able to avoid all collisions within its urban city operations. Using a LIDAR based sensor package to essentially create a 3D map, *Kwatee* is able to visualize all buildings, structures, and other aircraft in its vicinity that are outside its 3 meter box. *Kwatee* also integrates data from thermal sensors and an optical/IR camera to improve its autonomous flight in all directions.
- **Flight Navigation and Communication (GNC):** Using both a SATCOM and radio transponder, *Kwatee* is able to send and receive data through a real-time feed, either in LOS or BLOS. This datalink is sent to the Ground Station for operators to obtain important data, or sent to ATC and other aircraft (necessary for FAA mandated Automatic Dependent Surveillance – Broadcast or ADSB). In order to properly share the airspace, the sensor suite contains an integrated TCAS II system (Traffic Collision and Avoidance). *Kwatee* also uses satellite technology to determine accurate positioning and location in order to reach the designated target. Using a dual GPS and GNSS receiver and sensor drift correction, the aircraft's position is obtained with a precision around  $\pm 1$  in.
- **Takeoff and Landing:** For autonomous take-off and landing, *Kwatee* has precise measurement of height above ground level. Using a radar altimeter for longer range readings and a LIDAR for readings close to the ground (reduced uncertainty), the vehicle accurately assesses its height and determines if any obstructions are in the way of a safe landing.

- Supporting Equipment:** *Kwatee* also contains a variety of equipment necessary for VRF flight (MFR Minimum Equipment List). These include but are not limited to tachometers, engine temperature gauges, oil pressure gauges, fuel gauges, emergency locator transmitter, and navigation lights. In addition, the aircraft is fitted with a variety of equipment to help its longevity and efficiency in flight such as hall-effects sensors, strain gauges, cooling system, circuit breakers and other performance sensors. Lastly, the aircraft contains a 12 V Lithium Ion start-up battery used to provide full power to all the electronics.

Figure 10.1 lays out the system architecture of the avionics on board *Kwatee*. The chart displays the interaction of each component of the avionics.

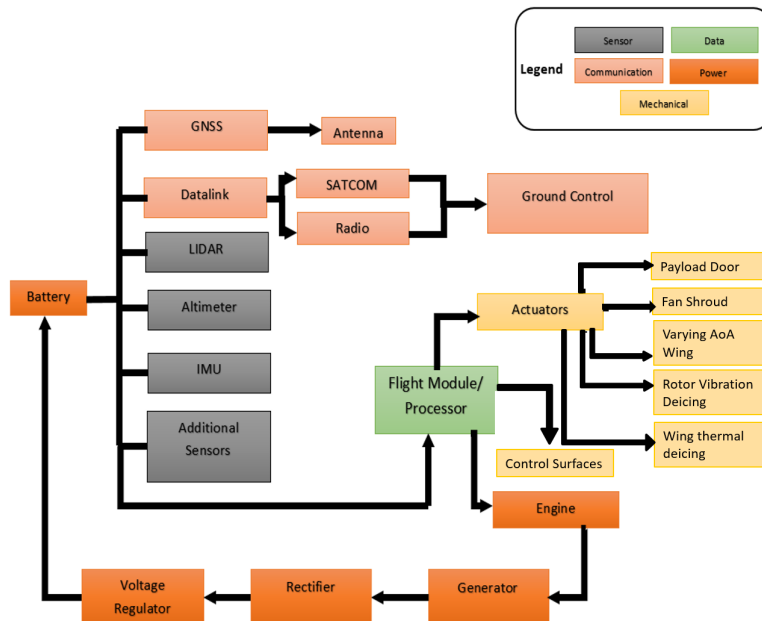


FIGURE 10.1: Avionics Flow Chart

## 10.2 Sensor Suite

The main qualities evaluated for sensor selection are compactness, minimal weight and reduced power consumption to make *Kwatee* as efficient as possible while meeting all the requirements to complete the mission objectives. The suite also incorporates redundancy and system monitoring to account for any malfunctions in equipment and the necessary adjustments that need to be made.

### 10.2.1 Flight Control and Autonomy

- Cloud Cap Technology Piccolo II- Flight Module/Autopilot and IMU:** This integrated avionics solution contains flight control processor, inertial sensors, and ported air data sensors, as well as a variety of essential software packages used to create feedback loops and configure aircraft data for unmanned flight. The IMU (Inertial Measurement Unit) integrated into the module contains a combination of inertial sensors (INS and gyros). It accomplishes 11 degrees of freedom through the 3-axis linear degrees of freedom (DOF) accelerometer, 3-axis gyroscopic, 3-axis magnetometer, 1 for temperature sensing and 1 DOF for pressure sensing. The module

itself inputs measurements from the various on board sensors (LIDAR, pitot-static, etc.), then processes the data using control algorithms and software packages, and lastly outputs the flight data to the actuators to determine the maneuvers the aircraft must make, thus making it a full autopilot module. *Kwatee* will also contain an independent **MTi 100-series** IMU for redundancy in case of flight module failure.

- **TSI 634000 Pitot Static and Temperature Sensor:** This sensor measures air speed and temperature to determine what adjustments need to be made to the engine output and RPM.
- **Puck VLP-16 LIDAR Sensor:** Used for obstacle sensing and avoidance, LIDAR sensor can scan 300,000 points per second to generate a three-dimensional point data cloud with a 100 m (328 ft) range and 3.0 cm (1.2 inch) accuracy on a 120 degree horizontal field of view. In hover, 4 LIDAR sensors around the fuselage can detect anything outside 3 meter circle to allow for tight hover movements in an urban canyon environment (Figure 10.2). In forward flight, LIDAR is mounted on the nose to detect obstructions in front of aircraft. Finally, during take-off and landing, LIDAR sensor is used to gain an accurate measurement of aircraft altitude above ground. Puck VLP LIDAR are some of the most compact on the market (.363 kg each).

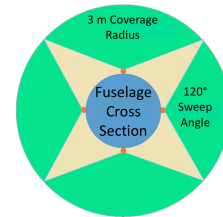


FIGURE 10.2: LIDAR Sweep to a 3 m Diameter

### 10.2.2 Flight Navigation and Communication

*Kwatee* has a diverse communication suite used to successfully relay data to ATC or other aircraft. A GNSS transmitter and associated antennae (x2) uses a multi-channel receiver to provide *Kwatee* with precise position accuracy required for hover during the mission, which are beyond that of a traditional GPS. *Kwatee*'s **NovAtel's OEM GNSS Transmitter/ Receiver** uses multi-frequency tracking on 220 different channels and features flexibility power consumption, upgradeable software and comprehensive message suites for ease of configuration and data logging. This GNSS system will measure *Kwatee*'s location to a precision of ( $\pm 2.54$  mm). A back up **Trimble Force 524D** is used in case of GNSS failure, but is not as precise compared to the GNSS platform ( $\pm 61$  cm). In case of poor GPS signal, *Kwatee* is able to fully navigate at a constant altitude using only its INS system until the satellite signal is regained.

To facilitate LOS communication in VHF UHF frequencies, *Kwatee* uses **UAV Navigation PSY90081 Radio Datalink** at a range of 185 km (100 nm) to operate remote missions while still maintaining proper communication. It also has Mode S capabilities and uses FAA mandated ADSB technology, required by 2020 in order to send data to other aircraft and ATC.

In a city environment it is essential that communication is made when the aircraft is beyond LOS. Using satellite communication with an **AC-27 SATCOM Datalink and Antenna**, enables the aircraft to be monitored over its datalink through a small delay. The Ku-band system enables operators to transmit and receive data over 204 km (110 nautical miles) at 45 MB/sec.

### 10.2.3 Take-Off and Landing

- **GRA 55 Radar Altimeter:** This altimeter will be used to determine aircraft altitude above ground level while in hover or forward flight. This RADALT measures altitude above the ground from 0 to 777 m (2,550 ft) while in forward flight with 1.5 m (5 ft) accuracy. Its function is to

assist the pitot-static probe and GNSS in getting altitude data while the aircraft flight control integrates the data.

- **FLIR MLR-4K LIDAR Sensor:** This light weight LIDAR range finder has a maximum measuring range of 90 m (300 ft) in high reflectivity (90%) and 56 m (185 ft) at low reflectivity (18%). The LIDAR achieves 10 cm (4 in) accuracy, allowing for safe and precise landing maneuvers and take-off maneuvers, as *Kwatee* approaches close to the ground.

#### 10.2.4 Supporting Equipment

- **VFR MEL:** The FAA mandates that all aircraft have a certain minimal equipment package necessary for all VFR flight. Aside from the equipment already mentioned that would be a part of this list, the flight sensors for Day VFR flight include temperature sensor, barometric pressure sensors, control surface position sensors, landing gear position sensors, fuel level sensors, and oil pressure gages. Within this package there will also be sideslip angle and AoA probes, used especially during transitional flight to determine safe transition between hover and forward flight. For safety, *Kwatee* will also be equipped with an emergency locator transmitter (ELT) and aviation anti-collision light system.
- **Engine Performance Sensors:** These sensors are used to evaluate the state of components within the engine assembly to determine its condition during flight. The **TE Connectivity Ni1000SOT** is used to monitor temperatures of each engine to feed information to the flight controller to determine if RPM needs to be dropped. The **Eaton DCCS50-100** sensor uses a hall-effect sensor package that measures changes in the magnetic field created by current flow in the wire passing through the aperture. The flight controller can then identify performance and damages based on data spikes.
- **Primary 12 Volt Lithium-Ion Batter:** This battery is used to start the engine and to redundantly power the avionics and controllers within the aircraft. Should a main power loss occur, this battery would enable the pitch actuators and avionics to continue working during the emergency landing. Li-Ion battery allows for versatile starting temperatures (as low as  $-10^{\circ}\text{F}$  /  $-23^{\circ}\text{C}$ ) as well as a high specific energy (100–265 W·h/kg).
- **Rigid 36762 Micro Switch:** A digital output switch to determine if the payload door is closed completely; to allow *Kwatee* to know the payload package is stowed safely and is ready to take-off.

##### 10.2.4.1 Avionics for Morphing and Reconfigurability

When *Kwatee*'s box wing changes its pitch angle, there are two main sensors that monitor the movement of the actuators. The first is a Hall effect sensor, used for proximity switching while the wing moves. Using a semi-conductor on *Kwatee*'s fuselage and a magnet on the wing, the Hall effect sensor can determine whether the wing has successfully actuated to its proper position, at a given distance away from *Kwatee*'s body. Secondly, a linear potentiometer is used to measure the distance undergone by the linear actuating strut. As the actuator moves along the strut, the potentiometer measures the linear distance using a resistive element, thereby measuring the proper distance the actuator must move to tilt the wing to a pitch range of  $\pm 5^{\circ}$ .

In addition to the wing, the motor controlling the shroud door on the fan is governed by a shaft encoder. This shaft encoder converts the angular position or motion of the shaft to an analog signal, providing information to the flight controller that the fan door is open and ready to be used.



### 10.3 Optional Equipment

*Kwatee* uses a variety of optional equipment, based on its current mission and necessities during flight. These pieces of equipment are removable and can be easily changed out or put on if it is necessary before its mission, thus, they are considered as payload mass only and empty weight. The following would be included as optional equipment:

- **BOSON 320 Thermal Sensors:** Quark 640 thermal imaging cameras around the fuselage will be able to provide improved awareness of moving obstacles such as birds or aircraft based on their heat signature, both during hover and forward flight.
- **Vision CM202 Gimbaled Camera:** This camera package is a gyro-stabilized, multi-sensor unit capable of 2 degree of freedom rotation to help analyze and survey images below and in front of *Kwatee* at a 120 degree field of view. This sensor would most likely be used for any type of surveillance missions performed by *Kwatee* where *Kwatee* must map out and survey a piece of land to determine information. The package uses an IR sensor with a max range of 500 ft (153 m) at 4 in (10 cm) accuracy. The LIDAR aids in collision avoidance while in forward flight and acts as a redundancy to the already existing LIDAR. It also uses an optical camera with a data feed to be sent to a ground station for image processing. And finally an IR sensor for little or no light flight conditions to help in a safe flight.
- **Sparton LPC-500 Processor/ Storage:** This CPU and storage module would be used for extra processing power to speed up calculations and SLAM algorithms, in addition to containing 1 TB of extra storage. It includes an internal cooling fan and temperature monitoring as well, to facilitate cooling and early warning in the case of overheating.

### 10.4 Placement of Avionics

Avionics were strategically placed around the vehicle to maximize their effectiveness. The placement of avionic components can be seen in Figure 10.1.

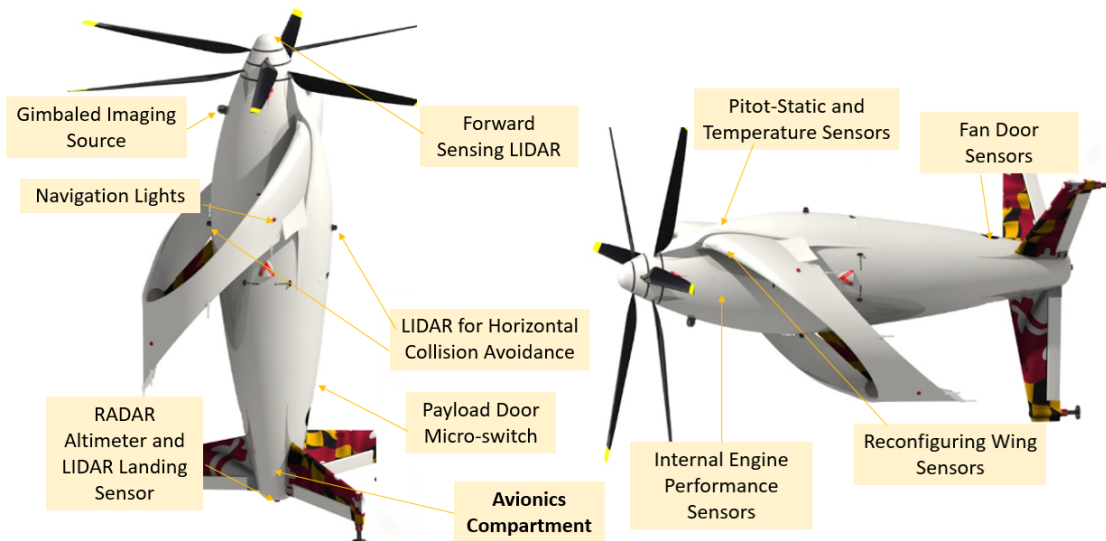


FIGURE 10.3: Avionic Placement



## 10.5 Avionics Weights and Power Requirements

The avionics for *Kwatee* have been selected to ensure a lightweight and effective avionics suite that is affordable to the customer. To do this, technology that has been tested and documented has been selected to fly on *Kwatee*. A breakdown of the avionics weights along with their power requirements are shown in Table 10.1. The total power requirement of the Avionics suite is 213 W, it's weight is 16.63 kg and the total cost is \$17,920.

TABLE 10.1: Avionics Breakdown

Component	Model	Qty	Unit Weight (kg)	Total Weight (kg)	Unit Power (W)	Total Power (W)	Unit Cost (USD)	Total Cost (USD)
<b>Fight Control</b>								
Flight Module and IMU	Cloud Cap Piccolo II	1	0.64	0.64	5	5	5,000	5,000
IMU	MTi 100-Series	1	0.34	0.34	0.9	0.9	1,200	1,200
Pitot-Static/Temp Sensors	TSI 634000	4	0.09	0.36	0.5	2	50	200
LIDAR	Puck VLP-16	5	0.36	1.8	8	40	230	1,150
<b>Flight Navigation/Communication</b>								
GNSS Transceiver	NovAtel's OEM	1	0.54	0.54	8	8	1,000	1,000
GPS Transceiver	Trimble Force 524D	1	0.45	0.45	4	4	760	760
Radio Datalink Transceiver	UAV Navigation PSY90081	2	0.45	0.91	7	14	1,400	2,800
SATCOM Datalink	AC-27	1	0.53	0.53	20	40	3,100	3,100
<b>Take-Off and Landing</b>								
RADAR Altimeter	GRA 55	1	1.36	1.36	12	12	200	200
LIDAR	FLIR MLR-4K	1	0.11	0.11	8	8	30	30
<b>Supporting Equipment</b>								
VFR MEL	-	-	-	2.27	-	20	-	1,500
Primary Battery	12 V Lithium Polymer	1	3.67	3.67	-	-	150	150
Engine Temperature Sensor	Connectivity Ni1000SOT	2	0.23	0.46	4	8	150	300
Engine Performance Sensor	DCCS50-100	2	0.09	0.18	5	10	160	320
Navigation and Landing Lights	-	5	0.45	2.25	5	25	15	75
Payload Door Micro-switch	Rigid 36762	1	0.2	0.2	2	2	25	25
Hall Effect Sensor	RH152	2	0.03	0.06	5	10	30	60
Linear Potentiometer	LPPS-22	1	0.3	0.3	2	2	25	25
Shaft Encoder	CUI AMT1	1	0.2	0.2	2.5	2.5	25	25
<b>Total</b>				16.63 kg (36.66 lbs)		213 W (.286 hp)		\$17,920

# Flight Dynamics and Control

The RFP requires that the aircraft must be “controllable and stable at all times” through its flight. *Kwatee* is designed to operate in hover and forward flight, with a transition to and from each mode, and its control scheme has been developed to maintain stability of the aircraft at all times.

## 11.1 Flight Dynamics Model

*Kwatee's* flight dynamics model depends on which flight mode it is operating in: while in hover *Kwatee* behaves as a helicopter but in forward flight *Kwatee* functions as a fixed-wing aircraft. The main features of *Kwatee* that affect its in-flight behavior include the coaxial rotors, the variable incidence box-wing, the vertical tail and V-tail, the fan in the fuselage, and the control surfaces on the wings and tails. Each component exists to provide a beneficial force or control moment at some point during flight, if not during all points of flight. Free-body diagrams of *Kwatee* in hover and forward flight are shown in Figures 11.1 and 11.2.

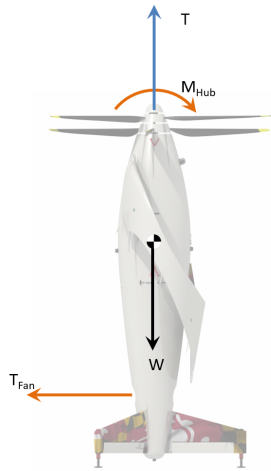


FIGURE 11.1: Hover

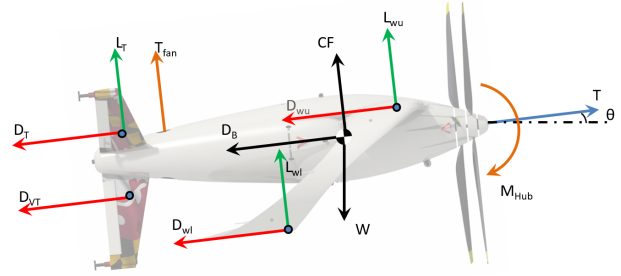


FIGURE 11.2: Forward Flight

## 11.2 Control Scheme

The maneuvers of *Kwatee* in hover, transition, and forward flight (in airplane mode) are described in this section.

### 11.2.1 Hover and Forward Flight Maneuver

TABLE 11.1: Mechanisms for Desired Maneuvers

	Pitch	Roll	Yaw
Hover	Cyclic	Cyclic	Differential torque of coaxial proprotors
Forward Flight	Elevators	Flaperons	Rudder

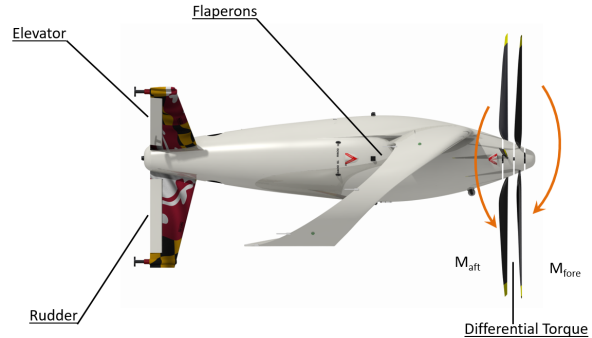


FIGURE 11.3: Locations of Control Mechanisms

The presence of the box wings which are in the downwash field of the rotor can cause the vehicle to be sensitive to gusts. To avoid this gust sensitivity, the wings have the ability to change their angle of attack so that they generate zero lift. It is then possible to orient the wings so that no moment resulting from lift of the wings is produced in hover. The variable incidence wings also provide benefit to transition as shown in Section 11.2.2.

### 11.2.2 Transition

The RFP requires *Kwatee* transition from hover to forward flight and vice versa and that the aircraft must be stable and controllable throughout flight. Possible transition maneuvers are either a stall-tumble maneuver or a continuous ascent. The stall-tumble is a relatively quick maneuver but creates

the risk of losing control of the aircraft due to stall and does not satisfy the RFP. Based on the controller design proposed by Jung and Shim[12], *Kwatee* employs the continuous-ascent maneuver to transition from hover to forward flight, and vice versa (Figure 11.4). An improved version of this method of transition has been developed using the variable incidence wings and bidirectional ducted fans.

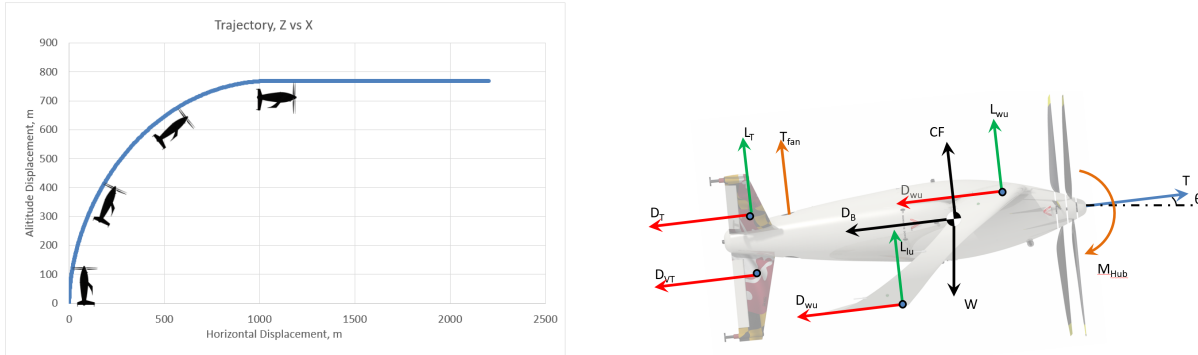


FIGURE 11.4: *Kwatee*'s Continuous-ascent Transition and Transition Free Body Diagram

In this novel control scheme, variable incidence wings and bidirectional ducted fans are used to keep power consumed at a minimum and maintain axial flight. A change in body pitch angle is mainly accomplished by the bidirectional ducted fans in the fuselage supplemented, if necessary, by a small cyclic of the rotors. Since the moment arm of the fan is large, the power needed to generate a body pitching moment is low. In order to maintain the desired transition path, the variable incidence wings are used to moderate the centrifugal force that the aircraft experiences while in the smooth transition maneuver.

The force and moment equilibrium equations at any point on the trajectory are shown in Figure 11.4 and written in equations 11.1, 11.2, and 11.3.

$$mV_i \frac{d\theta}{dt} = mg \cos \theta - \frac{1}{2} \rho S V_{i-1}^2 C_L \quad (11.1)$$

$$m \frac{dV}{dt} = T - \frac{1}{2} \rho S V_i C_D - mg \sin \theta \quad (11.2)$$

$$L_{wu} e_{wu} + M_{wu} - L_{wl} e_{wl} + M_{wl} - L_T e_T + D_{wu} d_{wu} + D_T d_T + D_{vt} d_{vt} + M_{control} = I \frac{d^2 \theta}{dt^2} \quad (11.3)$$

Where  $m$  is *Kwatee*'s mass,  $V_i$  is the velocity at time  $t = i$ ,  $V_{i-1}$  is the velocity of at time  $t = i - 1$ ,  $\frac{d\theta}{dt}$  is the body pitch rate,  $g$  is Earth's gravitational constant,  $\theta$  is the body pitch angle,  $\rho$  is the air density,  $S$  is the wing area,  $C_L$  is the coefficient of lift for the wing,  $\frac{dV}{dt}$  is the axial acceleration,  $T$  is the thrust,  $C_D$  is the coefficient of drag of the wing,  $L_{wu}$  and  $M_{wu}$  are the lift and pitching moment of the upper wing,  $L_{wl}$  and  $M_{wl}$  are the lift and pitching moment of the lower wing,  $L_T$  is the lift produced by the horizontal tail,  $e_i$  is the moment arms of  $L_i$ ,  $D_{wu}$  is the drag of the upper wing,  $D_{wl}$  is the drag of the lower wing,  $D_T$  is the drag of the horizontal tail,  $D_{vt}$  is the drag of the vertical tail, and  $d_i$  is the lateral moment arm of  $D_i$ .

The method of solution for the continuous-ascent was carried out using a time-stepping method and started by specifying a constant body pitch rate,  $\frac{d\theta}{dt}$ , and an initial velocity (Figure 11.5).

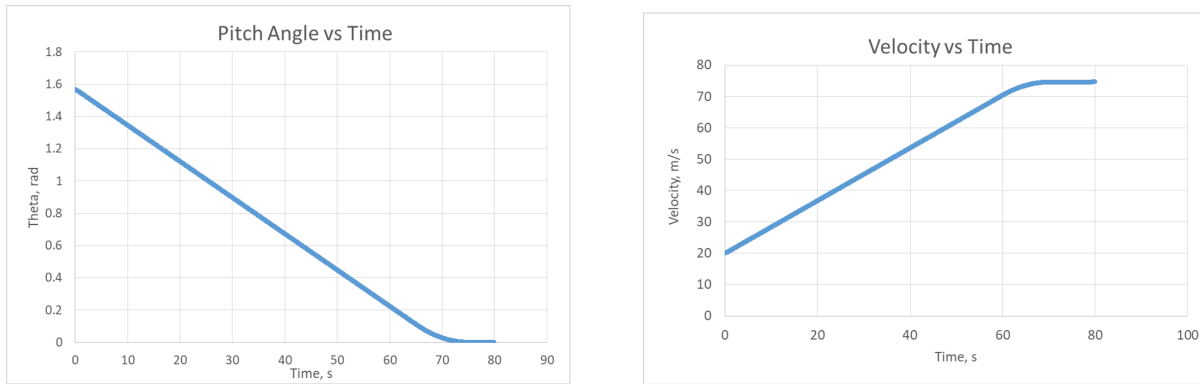
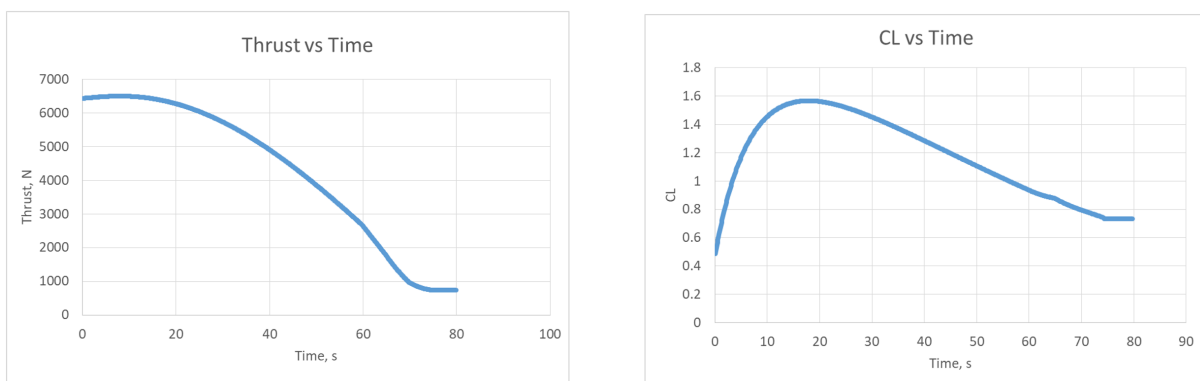


FIGURE 11.5: Body Pitch Angle (a) vs time and Velocity vs time (b)

From Equation 11.1,  $V_i$  is calculated from  $V_{i-1}$  and the axial acceleration,  $\frac{dV}{dt}$ , is calculated from,  $\frac{dV}{dt} = \frac{V_i - V_{i-1}}{\Delta t}$ . The resulting body pitch angle and velocity versus time are shown in Figure 11.5 for a 70 second transition. From Equation 11.2, the thrust required by *Kwatee* at every point during the transition maneuver can be calculated (Figure 11.6). Since  $\frac{d\theta}{dt}$  is known, Equation 11.3 will yield the required control moment (the sum of bi-directional ducted fan and rotor cyclic moments) for this maneuver.

The variety of possible transition maneuvers is constrained by the maximum allowed values of  $C_L$  because the wing flaperons are used in this transition in addition to the variable incidence wings. The body pitch rate and initial velocity must be adjusted so that  $C_L$  remains within the range of  $-1.2 < C_L < 1.6$  (Figure 11.6). In a location where restricted airspace may limit operating altitude, a tighter maneuver (less altitude gain and horizontal displacement) is possible but higher wing incidence angles are required in order to maintain the range of  $C_L$  values.

One possible transition maneuver is shown in Figures 11.5 and 11.6. Figure 11.5(a) shows the body pitch angle as a function of time when  $\frac{d\theta}{dt}$  is specified so that the maneuver is completed in 70 seconds. Figure 11.5(b) shows that, starting from an initial velocity of 72 km/h, the vehicle can reach 281 km/h in the same time. The thrust as a function of time is shown in Figure 11.6(a); it varies from a climb in hover of 7000 N to 740 N. Finally, Figure 11.6(b) shows the variation of  $C_L$  vs time.

FIGURE 11.6: Required Thrust vs time (a) and  $C_L$  vs time (b)

The reverse maneuver, from level forward flight to hover, follows the same method as the hover to forward flight transition maneuver. *Kwatee* will begin at low altitude and pitch upwards at a specified

rate until hover is achieved. Once in hover, *Kwatee* will descend to its landing destination. Similar to the hover to forward flight transition, tighter maneuvers can be accomplished if a larger range of wing incidence angles are available. The entire flight path that *Kwatee* will cover is shown in Figure 11.7

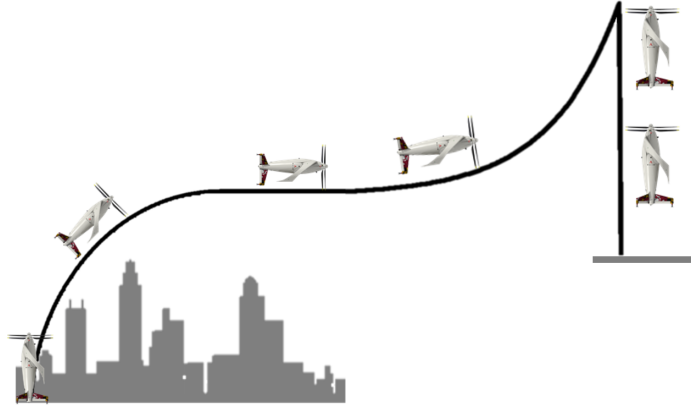


FIGURE 11.7: *Kwatee's* Complete Flight Path

### 11.3 Empennage Sizing

The purpose of the empennage is to balance the moments produced by the wing and fuselage. The size of the horizontal tail is directly proportional to the amount of lift produced by the tail and its moment arm. The empennage is initially sized using the tail volume coefficient (the V-tail is treated as having a vertical and horizontal tail components). The tail volume coefficients are defined as

$$c_{vt} = \frac{L_{vt}S_{vt}}{b_w S_w} \quad (11.4)$$

$$c_{ht} = \frac{L_{ht}S_{ht}}{C_w S_w} \quad (11.5)$$

where  $c_{vt}$  is the vertical tail coefficient,  $L_{vt}$  is the lift of the vertical tail (required to balance the moment produced by the wing in steady flight),  $S_{vt}$  is the area of the vertical tail,  $b_w$  is the span of the wing and  $S_w$  is the area of the wing,  $c_{ht}$  is the horizontal tail coefficient,  $L_{ht}$  is the required lift of the horizontal tail (for steady flight),  $S_{ht}$  is the area of the horizontal tail, and  $C_w$  is the wing mean chord. Using historical data from Raymer [9],  $c_{vt}=0.04$  and  $c_{ht}=0.6$ , the required area of the vertical tail was found to be  $0.118 \text{ m}^2$  and of the horizontal tail to be  $0.443 \text{ m}^2$ . The actual area of *Kwatee's* vertical tail is  $0.453 \text{ m}^2$  and of horizontal tail is  $0.444 \text{ m}^2$ . As mentioned previously the tail is designed primarily for landing purposes and although the "horizontal tail" matches closely with initial sizing, the *Kwatee's* vertical tail area is much greater than initial sizing suggests. From Raymer [9] the ailerons will cover 66% of the wing's span and 27% of the chord. Elevator and Rudders will cover from fuselage to 97% of the tail's span and 27% of the tail's chord. These ranges were taken into account when designing the control surfaces used in forward flight but they may be adjusted once wind tunnel or small model testing are conducted.

### 11.4 Static Stability

How an aircraft responds in pitch to a change in angle of attack is a measure of its static longitudinal stability. The aircraft naturally accomplishes this through the moments present on the aircraft, mainly from the wings and the horizontal tail. As shown by Lutze[13], longitudinal static stability can be indicated by the inequality,

$$\frac{dC_m}{d\alpha} < 0 \quad (11.6)$$

where  $\frac{dC_m}{d\alpha}$  is the longitudinal stability parameter. The longitudinal stability parameter can be calculated following Raymer [9], starting with moment equilibrium about the center of gravity,  $M_{cg}$ .

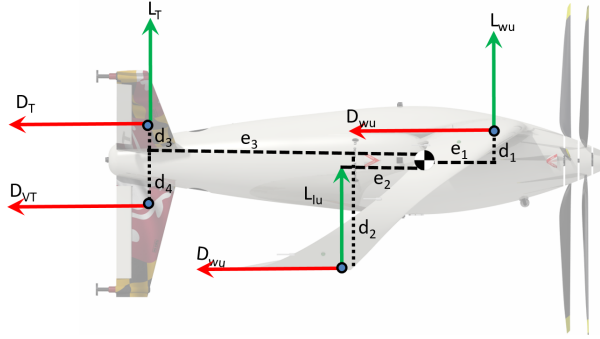


FIGURE 11.8: Moment Equilibrium for Static Stability

Expressing the moment equilibrium for static stability in non-dimensional form Eq 11.3 can be rearranged to,

$$C_{M_{cg}} = C_{L_{wu}} \frac{e_{wu}}{c_{wu}} + C_{M_{wl}} - C_{L_{wl}} \frac{e_{wl}}{c_{wl}} + C_{M_{wt}} - \eta_h \frac{S_h}{S_w} C_{L_T} \frac{e_T}{c_T} \quad (11.7)$$

where  $\eta$  is the ratio of dynamic pressure experienced by the horizontal tail to wing (taken to be 0.9) and  $\frac{S_h}{S_w}$ , the ratio of horizontal tail and wing areas. Taking the derivative of each term with respect to angle of attack will yield an equation for the longitudinal stability parameter.

$$\frac{dC_M}{d\alpha} = C_{L_{\alpha_{wu}}} \bar{e}_1 - C_{L_{\alpha_{wl}}} \bar{e}_2 - \eta_h \frac{S_h}{S_w} C_{L_{\alpha_{ht}}} \frac{d\alpha_h}{d\alpha} \bar{e}_3 \quad (11.8)$$

where  $\bar{e}_i = \frac{e_i}{c}$  and  $\frac{d\alpha_h}{d\alpha}$  accounts for downwash effects caused by the wings that influence the actual angle of attack of the horizontal tail. Using approximations for terms in Eq 11.8 from Lutze[13],  $C_{M_{\alpha}}$  is found to be negative, satisfying the requirement for longitudinal stability. Location of the center of gravity along the longitudinal axis is crucial to longitudinal static stability as it directly affects the magnitude of the moments generated by the lifting surfaces. If *Kwatee's* center of gravity moved closer to its nose the stabilizing moment produced by the horizontal tail would be larger than the current design, resulting in a more stable aircraft. Fuel consumption during flight moves the center of gravity forward about 0.38 m but this does not adversely affect the stability.

## Acoustics

*Kwatee* is designed for civilian missions and therefore must meet the FAA defined noise requirements (FAA Section J36.305 Noise Limits). For a helicopter that is at the RFP MTOW of 600 kg, the upper limit for noise is set at a fixed 82 dB.

Loading noise is directly related to the amount of thrust within a given area. With *Kwatee* being a tailsitter, in axial flight there will be a great reduction in noise due to the lack of unsteady loading noise, or blade vortex interactions. With traditional helicopters, this noise needs to be taken into consideration for those on the ground. While *Kwatee* is in axial flight, instead of being directed downward, the loading noise will be directed towards the front and rear of the aircraft contributing only a small amount of noise that affects those on the ground. For blade design purposes, the tip speed of the blades was limited to maintain a subsonic blade tip. Acoustically this helps with reducing the effects of thickness and high speed impulsive noise that originates from high Mach tip speeds.

During the design process, when prioritizing design drivers of *Kwatee* other aspects were placed higher in importance than the noise limits due to the mission profiles selected for this aircraft, however meeting the FAA certification requirements was placed as a design criteria.

## CONOPS

The *Kwatee* has been designed with a primary mission of emergency cargo delivery, however, the vehicle's versatility allows it to perform additional missions if configured to do so. The following details the Concept of Operations (CONOPS) for the aircraft.

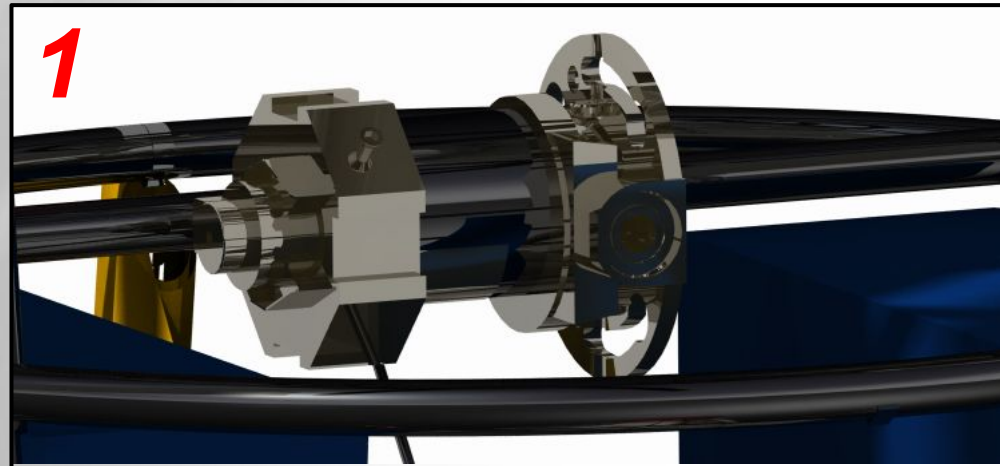
### 13.1 Basis for Concept of Operations

*Kwatee* is a Class 3 VTOL aircraft capable of maneuvering in tight spaces commonly found in urban canyons. *Kwatee* has been designed to offer an exceptional balance between hovering and forward flight performance metrics, but it is also capable of superior cruise of up to 263 km/h (142 knots) for best range at 3,000 m. This high cruise speed can reduce the time during emergency supply and disaster relief missions. Although propulsive efficiency is slightly compromised in this case, *Kwatee* is a solution for emergency response, specifically when lives are at stake.

### 13.2 Cargo Loading

Payload loading and unloading is done with the assistance of human interaction on the ground. To load the *Kwatee*, the payload door is opened via a handle that sits approximately five feet off the ground. Gravity pulls the door open while two steel cables stop the door at the appropriate angle for loading. Once open, those receiving the payload remove two manually locking pins from two sets of load bearing steel telescoping rails. The rails are then manually extended until they reach the ground, at which point the two locking pins are re-inserted into the rails to keep them in position. A 2224 N (500 lbf) winch rests inside the fuselage ready to pull the payload up and into the cargo bay via a steel cable with brass hook on the end. The hook is connected to the handle on the payload box, and then the ground support will operate a small remote that is fastened to the inside of the payload door, activating the winch and pulling the payload into the cargo bay. The cargo bay dimensions are designed to hug the payload so that it will not jostle during flight. Once the payload is inside the vehicle, the locking pins will be removed, the rails retracted back to their original positions, the pins inserted back into the rails, and the payload door pushed shut by ground support. Unloading *Kwatee* follows the same process, with the exception of simply using the remote to lower the payload. A detailed representation of the loading and unloading process, is shown in the Payload Loading fold-out.

# Automated Payload Loading/Unloading

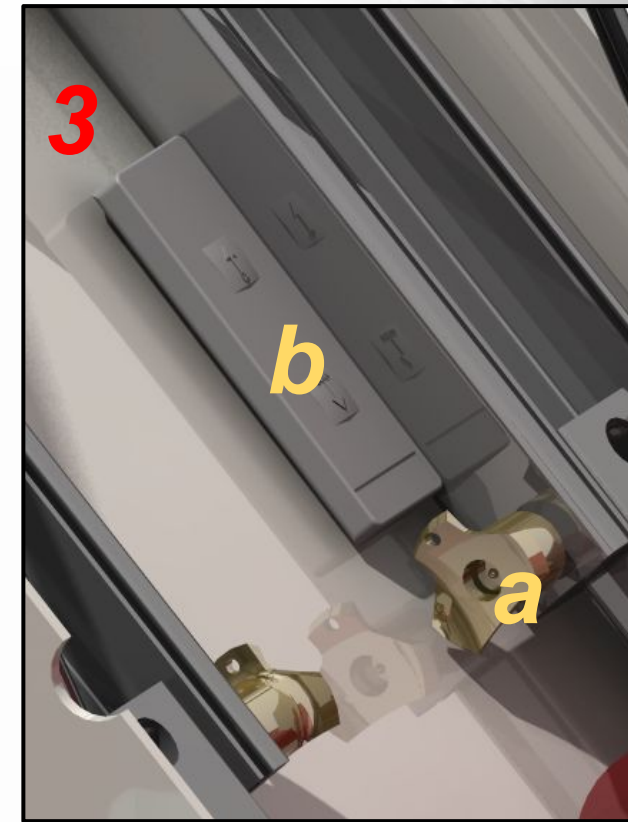
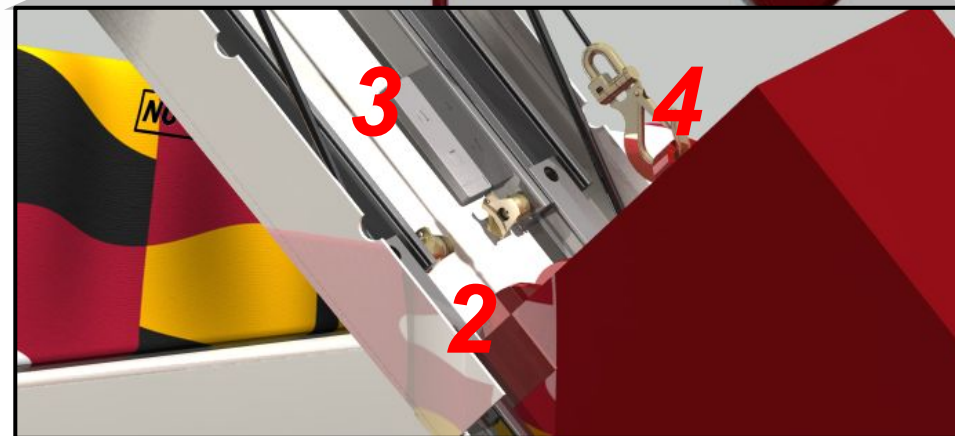
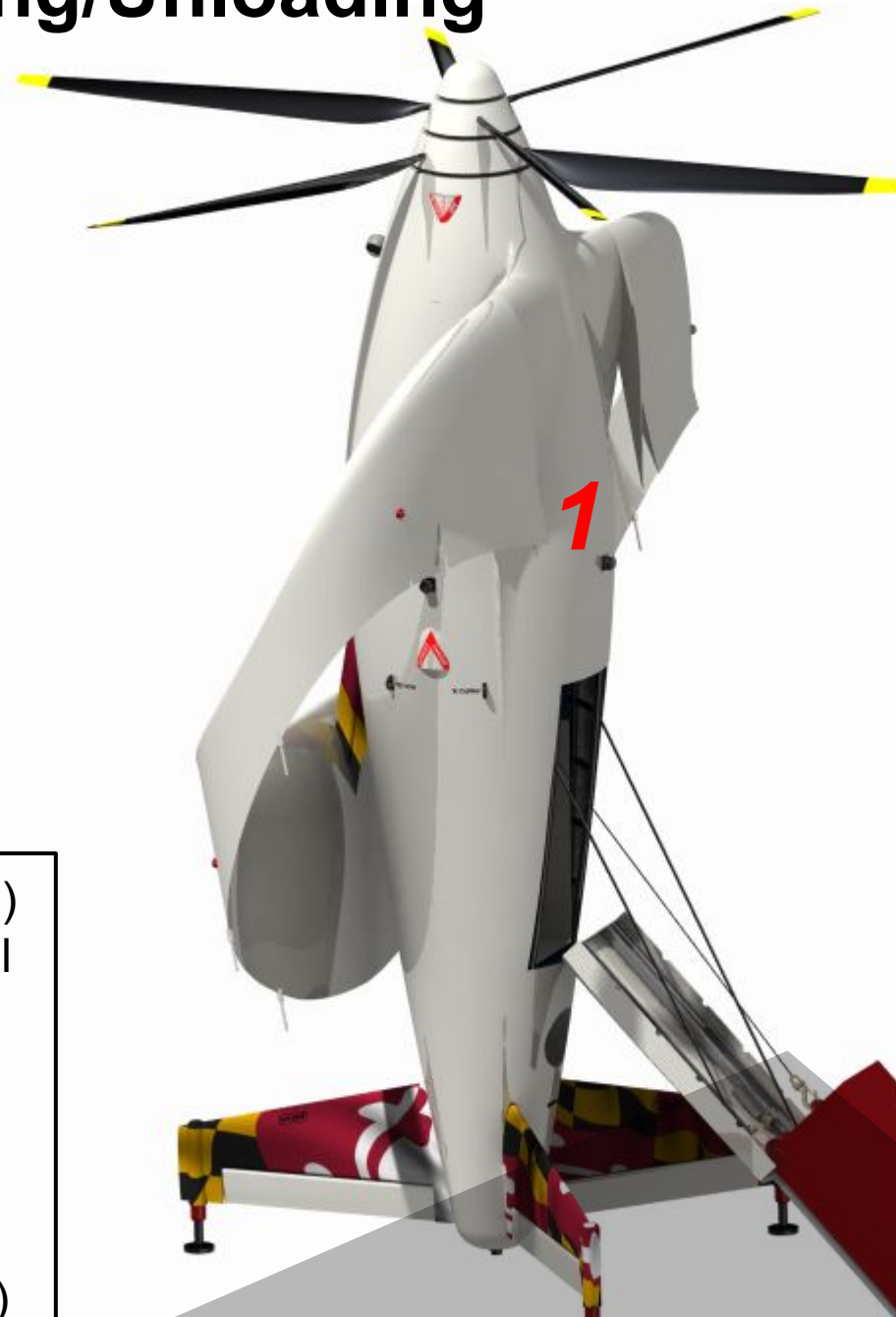


A 500 lbf (2224 N) max force rated winch pulls the payload via steel cable



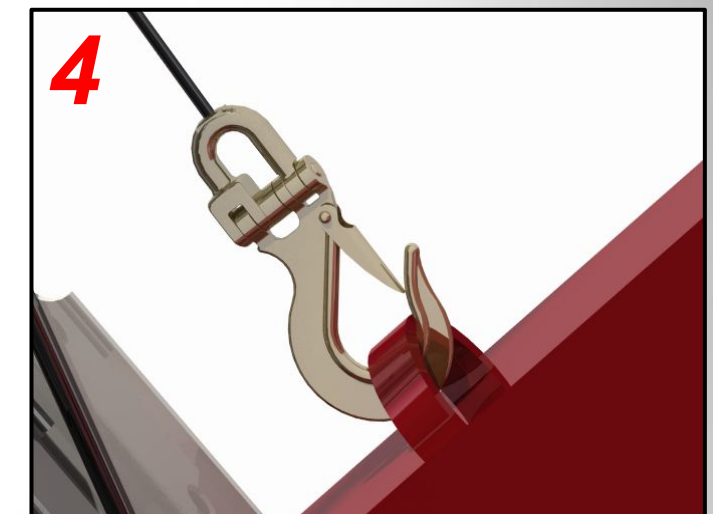
Two, 200 kg (441 lb) max load rated steel rails (a) can telescope out to twice their original length.

Two steel cables (b) control the angle that the payload door makes rotating about its hinge, allowing for a 40° angle of climb for the payload.



Two brass pins (a) secure the telescoping rails in both the retracted and extended positions.

A remote control (b) is attached to the payload door and is used to operate the winch.



A brass hook is manually attached and removed from the payload during loading.



### 13.3 Intelligence, Surveillance, Reconnaissance (ISR)

*Kwatee's* unmanned operations make it capable of Intelligence, Surveillance, and Reconnaissance missions that may be too dangerous for manned operations. *Kwatee* is capable of providing rapid response and monitoring of disasters such as Hurricane Harvey, the storm that greatly affected eastern Texas in 2017. Additionally, *Kwatee's* superior structural build allows researchers to operate the vehicle in thunderstorms for data collection.

### 13.4 Transportation and Ground Safety

The *Kwatee* contains four tie down rings around the fuselage allowing it to be secured to the ground when landed. These tie downs can ensure that the vehicle is not blown over by strong wind gusts, and can also be used during transportation.

### 13.5 Maintenance

Two doors exist on opposite sides of the engine bay which provide access to both Stuttgart engines for maintenance and inspection. These doors, shown in Figure 13.1 together with the payload door also provide access to the avionics located inside the aircraft. The engine bay doors are located at a height of about 3.5m, and therefore a technician will need a ladder to get access to these doors. To perform maintenance and inspection on the ducts in the aft of the vehicle, the rotating shroud can be opened to get access to the ducts. The oleo-pneumatic struts of the landing gear stick outside and hence are easily accessible for maintenance and inspection. An internal pressure of 12,411 kPa (1,800 psi) was chosen for the oleo to allow for servicing with standard compressors.



FIGURE 13.1: Door providing access to the engine bay

## Cost Analysis

### 14.1 Production Costs

*Kwatee's* production cost estimations are based off of NDARC Model and Bell Helicopter Cost Equations [14] assuming a total production quantity of 100 aircraft and a production rate of 10 aircraft per year. Two example equations are shown below

**Weight**= Weight of rotor system (lb)

**Kyokmat**: Yoke material factor

**Bldno**: Number of main rotor blades

**Kbldmat**: Blade material factor

**Prodq**: Total number to be produced

**Prodr**: Production rate [number/year]

**Average Main Rotor System Cost** =  $1,500 * \text{Weight}^{.7} * \text{Kyokmat} * \text{Bldno}^{.2} * \text{Kbldmat} * (\text{Prodq} * \text{Prodr})^{-.08}$

$$\text{Average Airframe Structure Cost} = 10,000 * \text{Weight}^{.8} * \text{Kmat} * (\text{Prodq} * \text{Prodr})^{-.13}$$

\* The total unit cost of *Kwatee* is \$496,400.00 using the inflation index from the U.S. Department of Labor in 2018 [15] to account for inflation between 2002 and 2018.

TABLE 14.1: Production Costs  
 \*\* Fuel cost based on prices as of May, 2018

Component	Cost
Blades and Hub	\$74,500
Fuselage Structure	\$42,000
Box Wing	\$30,000
Fins	\$3,500
Landing Gear	\$12,300
Fan and Shroud	\$500
Payload Door	\$8,000
Engine	\$160,000
Generator	\$5,200
Transmission	\$1,200
Fuel**	\$180
Cooling	\$850
Lubrication	\$210
Avionics	\$17,920
Inflation Index*	1.393
<b>Total</b>	<b>\$496,400.00</b>

*Kwatee's* total cost includes the development cost, production cost, operational cost, and end of life cost. While production costs can be seen in Table 14.1, the aircraft's operational cost will be kept relatively low, as all mechanical and electrical equipment on board are some of the newest and high-tech equipment on the civilian market, therefore maintenance would not be a frequent occurrence during the beginning of *Kwatee's* life-cycle. Additionally, with the ease of accessibility through the aircraft's hatches, all necessary repairable equipment can be done without removing the components themselves. Further considerations should be made for the cost of testing, other operational costs such as inspections and transportation, and end of life costs for non-recyclable components. *Kwatee* uses technology that is at a high readiness level. Using available technology lowers the expected testing and certification cost, keeping the overall cost of development to a minimum.

## Weight Breakdown

Throughout the design process, a table of weights was kept to maintain an accurate estimation about *Kwatee's* current weight. The final weight chart that is seen in Figure 15.1, tabulates all of the components of *Kwatee* as well as its location with respect to the aircraft's center of gravity.

*Kwatee* was designed to be as light weight as possible while still maintaining its high performance and versatile mission capabilities. *Kwatee's* structure is composed of light weight composite material, while its avionics were chosen for their light weight properties yet efficient capabilities. As the fuel tanks are located relatively close to the gross take-off CG, there is little CG movement as fuel burns, making flight control algorithms significantly easier to develop (Table 15.1).

TABLE 15.1: CG Position (From Top of Aircraft)

Full Fuel (100 kg)	Position of CG - <b>1.8 m</b>
50 % Fuel (50 kg)	Position of CG - <b>1.5 m</b>
No Fuel (0 kg)	Position of CG - <b>1.3 m</b>

\*\* Avionics Compartment Only



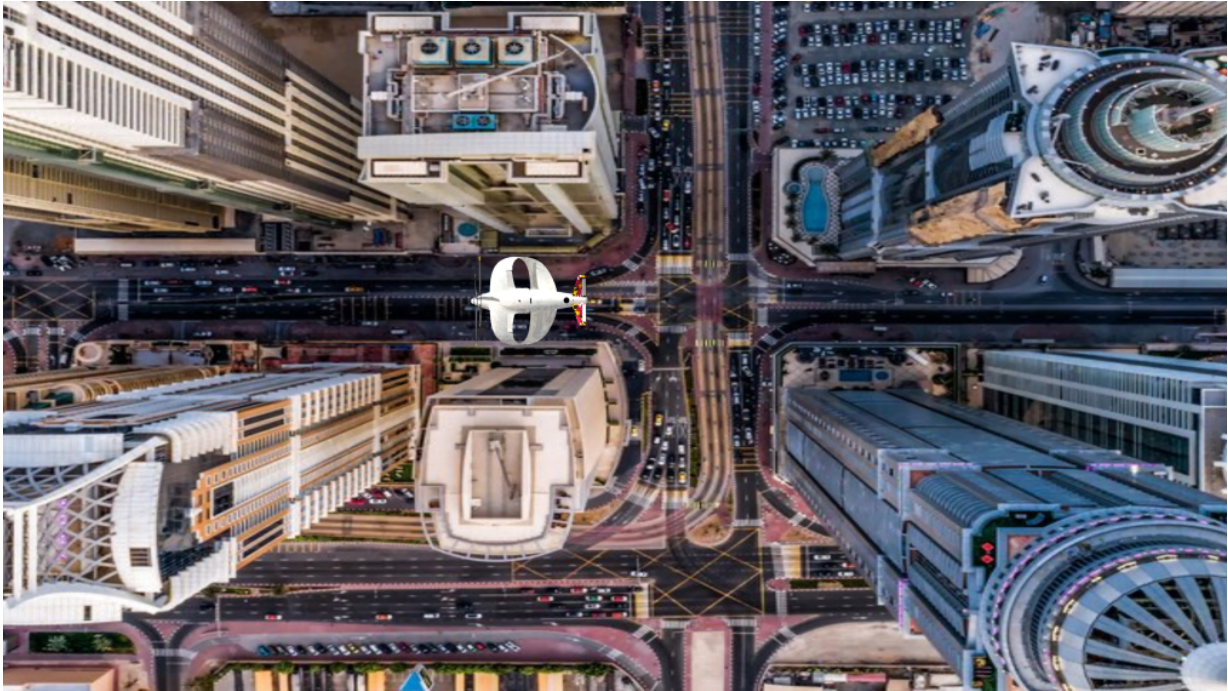
<u>CATEGORY</u>	<u>COMPONENT</u>	<u>WEIGHT (KG)</u>	<u>WEIGHT (LB)</u>	<u>% EMPTY</u>	<u>XCG (M)</u>	<u>XCG (FT)</u>
<b>FUSELAGE STRUCTURE</b>	Fuselage - Skin	20.23	44.60	6.10%	-	-
	Fuselage Airframe	30.25	66.69	9.13%	-	-
<b>WING</b>	Box Wing - Skin	23.71	52.27	7.16%	-	-
	Top Wing - Internal	14.71	32.43	4.44%	+0.81	+2.66
	Bottom Wing - Internal	14.73	32.47	4.45%	-0.72	-2.36
<b>ROTOR ASSEMBLY</b>	Connection Wing - Internal	4.35	9.59	1.31%	0.00	0.00
	Swashplate + Hub	8.04	17.73	2.43%	+1.65	+5.41
	Co-Axial Main Rotor- Skin	15.07	33.22	4.55%	+1.70	+5.58
	Co-axial Main Rotor - Internal	10.09	22.24	3.04%	+1.70	+5.58
<b>LANDING GEAR</b>	Landing Gear Assembly	3.12	6.88	0.94%	-2.20	-7.22
<b>PAYLOAD DOOR</b>	Payload Door System	24.78	54.63	7.48%	-0.83	-2.72
	Wench/Cable	4.11	9.06	1.24%	-0.83	-2.72
<b>FAN</b>	Fan Assembly	4.31	9.50	1.30%	-1.65	-5.41
<b>FINS</b>	Fin - Skin (X3)	5.21	11.49	1.57%	-1.85	-6.07
	Fin - Internal (X3)	21.01	46.32	6.34%	-1.85	-6.07
<b>CONTROL SURFACES/ACTUATORS</b>	Rudder/Elevator (on Fins)	1.50	3.31	0.45%	-2.10	-6.89
	Ailerons (on Wings)	7.03	15.50	2.12%	+0.30	+0.98
<b>ENGINE/PROPULSION ASSEMBLY</b>	Engine Assembly	60.07	132.43	18.13%	+1.03	+3.38
	Gear Box/ Transmission	10.01	22.07	3.02%	+1.09	+3.58
	Radiator/Lubrication/Cooling	5.03	11.09	1.52%	+1.05	+3.44
	Fuel Tank	17.31	38.16	5.22%	-0.48	-1.57
	Fuel Pump	10.07	22.20	3.04%	-0.48	-1.57
<b>AVIONICS/SENSORS</b>	See Section 10	16.63	36.66	5.02%	-1.96 **	-6.43 **
<b>EMPTY WEIGHT</b>	-	331.37	730.54			
<b>FUEL</b>	-	100.00	220.46			
<b>PAYLOAD</b>	-	100.00	220.46			
	<b>Total</b>	<b>531.37 kg</b>	<b>1171.47 lb</b>			
	Max	600.00 kg	1322.80 lb			

FIGURE 15.1: *Kwatee Weight Chart*

# Summary

In response to the Request for Proposal for the the 2017-2018 AHS Student Design Competition the University of Maryland's Undergraduate Team designed *Kwatee*, a coaxial box wing tail sitter. *Kwatee* is designed to meet and exceed design goals of the request of the proposal with the combined maneuverability of a helicopter with fast forward flight of a fixed wing aircraft into one versatile multi mission capable platform.

1. Novel variable incidence box wing to obtain optimal angle of attack in various flying conditions.
2. Utilize bidirectional ducted fan for efficient transition between flight modes.
3. Efficient hover, with figure of merit 0.782, capable of navigating megacities
4. Max dash speed of 426 km/h (230 knots), faster than comparable sized fixed wing aircraft.
5. Versatile multi-mission capable platform capable of many roles.
6. Extended range of 354 km (440 miles) allowing *Kwatee* to have a large service area.
7. Prolonged endurance 4.2 hours for prolonged search and rescue missions



# Bibliography

- [1] M. Tishchenko and V. T. Nagaraj, “ENAE634 Helicopter Design Lecture Notes.” University of Maryland, College Park, 2008.
- [2] “Polyurethane protective tape 8542hs.” 3M Corporation, November 2011.
- [3] Y. Wang, Y. Xu, and Q. Huang, “1. progress on ultrasonic guided waves de-icing techniques in improving aviation energy efficiency.” tech. rep., School of Aeronautic Science and Engineering, Beihang University, Beijing 100191, China.
- [4] N. Gupta and A. Karem, “U.S. Patent 7,972,114 B2,” March 2008.
- [5] S. Engineering, “Stuttgart STV130 Engines Specifications,” April 2018.
- [6] I. Kroo, “Nonplanar wing concepts for increased aircraft efficiency,” tech. rep., Stanford University, U.S.A, 450 Serra Mall, Stanford, CA 94305, 2005.
- [7] R. U. Prakash, G. R. Kumar, R. Vijayanandh, M. S. Kumar, and T. Ramganes, “Structural analysis of aircraft fuselage splice joint.,” dissertation, Department of Aeronautical engineering, Kumaraguru College of Technology, Coimbatore - 641049, Tamil Nadu, India.
- [8] J. Roskam, *Airplane Design, Part IV: Layout of landing gear and systems*. The University of Kansas, Lawrence: Cambridge University Press, 2004.
- [9] D. P. Raymer, *Aircraft Design: A Conceptual Approach. Third Edition*. No. pg 289, 1999.
- [10] J. Roskam, *U.S. Army, Engineering Design Handbook - Helicopter Engineering Part One: Preliminary Design (AMCP706-201)*,. 1974.
- [11] M. Nixon, “Aeroelastic response and stability of tiltrotors with elastically coupled composite rotor blades.” dissertation, Department of Aerospace Engineering, University of Maryland,, College Park, MD., 1993.
- [12] Y. Jung and D. H. Shim, “Development and application of controller for transition flight of tail-sitter uav,” tech. rep., Korea Advanced Institute of Science and Technology, August 2011.
- [13] F. H. Lutze, “Longitudinal aerodynamics estimating methods.” 2018.
- [14] V. T. Nagaraj, B. Govindarajan, and I. Chopra, *Helicopter Design*. To be published.
- [15] U.S. Department of Labor, “Consumer Price Index,” 2018.

